of multiple sclerosis patients undergoing immunomodulatory treatment. J Neurol Neurosurg Psychiatry 2003;74:123–6.
[9] Koike F, Satoh J, Miyake S, Yamamoto T, Kawai M, Kikuchi S, et al. Microarray analysis identifies interferon β-regulated genes in multiple sclerosis. J Neuroimmunol 2003;139:109–18.
[10] Šega S, Wraber B, Mesec A, Horvat A, Ihan A. IFN-β b1a and IFN-β1b have different patterns of influence on cytokines. Clin Neurol Neurosurg 2004;106:255–8.
[11] The PRISMS Study Group, UBC MS/MRI Analysis Group. PRISMS-4: long-term efficacy of interferon-β-1a in relapsing MS. Neurology 2001;56:1628–36.
[12] Ochi H, Mei F-J, Osoegawa M, Minohara M, Murai H, Taniwaki T, et al. Time-dependent cytokine deviation toward the Th2 side in Japanese multiple sclerosis patients with interferon beta-1b. J Neurol Sci 2004;222:65–73.
[13] McDonald WI, Compston A, Edan G, Goodkin D, Hartung HP, Lublin FD, et al. Recommended diagnostic criteria for multiple sclerosis: guidelines from the International Panel on the diagnosis of multiple sclerosis. Ann Neurol 2001;50:121–7.
[14] Kira J, Kanai T, Nishimura Y, Yamasaki K, Matsushita S, Kawano Y, et al. Western versus Asian types of multiple sclerosis: immunogenetically and clinically distinct disorders. Ann Neurol 1996;40:569–74.
[15] Picker LJ, Singh MK, Zdraveski Z, Treer JR, Waldrop SL, Bergstresser PR, et al. Direct demonstration of cytokine synthesis heterogeneity among human memory/effector T cells by flow cytometry. Blood 1995;86:1408–19.
[16] Ochi H, Osoegawa M, Wu X-M, Minohara M, Horiuchi I, Murai H, et al. Increased IL-13 but not IL-5 production by CD4-positive T cells and CD8-positive T cells in multiple sclerosis during relapse phase. J Neurol Sci 2002;201:45–51.
[17] Killestein J, Eikelenboom MJ, Izeboud T, Kalkers NF, Adèr HJ, Barkhof F, et al. Cytokine producing $CD8^+$ T cells are correlated to MRI features of tissue destruction in MS. J Neuroimmunol 2003;142:141–8.
[18] Terabe M, Park JM, Berzofsky JA. Role of IL-13 in regulation of anti-tumor immunity and tumor growth. Cancer Immunol Immunother 2004;53:79–85.
[19] Inoue Y, Konieczny BT, Wagener ME, McKenzie AN, Lakkis FG. Failure to induce neonatal tolerance in mice that lack both IL-4 and IL-13 but not in those that lack IL-4 alone. J Immunol 2001;167:1125–8.
[20] Bourreau E, Prévot G, Pradinaud R, Launois P. Interleukin (IL)-13 is the predominant Th2 cytokine in localized cutaneous Leishmaniasis lesions and renders specific $CD4^+$ T cells unresponsive to IL-12. J Infect Dis 2001;183:953–9.
[21] Ke B, Shen XD, Zhai Y, Gao F, Busuttil RW, Volk HD, et al. Heme oxygenase 1 mediates the immunomodulatory and antiapoptotic effects of interleukin 13 gene therapy in vivo and in vitro. Hum Gene Ther 2002;13:1845–57.

Available online at www.sciencedirect.com
SCIENCE DIRECT®
Biochemical and Biophysical Research Communications 343 (2006) 269–278
BBRC
www.elsevier.com/locate/ybbrc

Immunization with heat shock protein 105-pulsed dendritic cells leads to tumor rejection in mice ☆

Kazunori Yokomine [a,b], Tetsuya Nakatsura [a,*,1], Motozumi Minohara [c], Jun-ichi Kira [c], Tatsuko Kubo [d], Yutaka Sasaki [b], Yasuharu Nishimura [a,*]

[a] *Department of Immunogenetics, Graduate School of Medical Sciences, Kumamoto University, Kumamoto, Japan*
[b] *Department of Gastroenterology and Hepatology, Graduate School of Medical Sciences, Kumamoto University, Kumamoto, Japan*
[c] *Department of Neurology, Neurological Institute, Graduate School of Medical Sciences, Kyushu University, Fukuoka, Japan*
[d] *Department of Molecular Pathology, Graduate School of Medical Sciences, Kumamoto University, Kumamoto, Japan*

Received 18 February 2006
Available online 3 March 2006

Abstract

Recently, we reported that heat shock protein 105 (HSP105) DNA vaccination induced anti-tumor immunity. In this study, we set up a preclinical study to investigate the usefulness of dendritic cells (DCs) pulsed with mouse HSP105 as a whole protein for cancer immunotherapy in vivo. The recombinant HSP105 did not induce DC maturation, and the mice vaccinated with HSP105-pulsed BM-DCs were markedly prevented from the growth of subcutaneous tumors, accompanied with a massive infiltration of both $CD4^+$ T cells and $CD8^+$ T cells into the tumors. In depletion experiments, we proved that both $CD4^+$ T cells and $CD8^+$ T cells play a crucial role in anti-tumor immunity. Both $CD4^+$ T cells and $CD8^+$ T cells specific to HSP105 were induced by stimulation with HSP105-pulsed DCs. As a result, vaccination of mice with BM-DCs pulsed with HSP105 itself could elicit a stronger tumor rejection in comparison to DNA vaccination.

Keywords: Heat shock protein 105; Cancer antigen; Dendritic cells; Th; CTL

Heat shock proteins (HSPs) are soluble intracellular proteins, which are ubiquitously expressed, and their expression can be induced at much higher levels as a result of heat shock or other forms of stress. HSPs have essential functions in the regulation of protein folding, conformation, assembly, and sorting. HSPs have been shown to be molecular chaperones that function to maintain the native conformational states of proteins and prevent protein–protein aggregation [1]. HSPs can also induce the response of antigen-specific effector $CD8^+$ T cells which can protect hosts from both infection and tumor challenge [2]. Srivastava and co-workers [3,4] led to a proposal that the tumor-derived HSP–peptide complex elicits a protective immunity that is specific to a particular cancer, while HSPs derived from normal tissues did not elicit any protective immunity to the cancers tested. Immunotherapeutic clinical trials targeted at autologous tumor-derived gp96–peptide complexes are still ongoing in metastatic melanoma and colorectal carcinoma patients [5].

Dendritic cells (DCs) are powerful antigen-presenting cells (APCs) that are considered to be potent immunotherapeutic agents to promote the host immune response against tumor antigen. DCs become efficient tumor vaccines when pulsed with synthetic or natural tumor-derived peptides, transduced with tumor-derived RNA or vectors

☆ *Abbreviations:* BM-DC, bone marrow-derived DC; HSP105, heat shock protein 105; Th, helper T cell; CTL, cytotoxic T lymphocyte; MHC, major histocompatibility complex; C26 (C20), colon 26 clone 20.

* Corresponding authors. Fax: +81 96 373 5314 (Y. Nishimura); +81 4 7131 5490 (T. Nakatsura).
E-mail addresses: tnakatsu@east.ncc.go.jp (T. Nakatsura), mxnishim@gpo.kumamoto-u.ac.jp (Y. Nishimura).
[1] Present address: Immunotherapy Section, Investigative Treatment Division, Research Center for Innovative Oncology, National Cancer Center Hospital East, 6-5-1 Kashiwanoha, Kashiwa City, Chiba 277-8577, Japan.

0006-291X/$ - see front matter © 2006 Elsevier Inc. All rights reserved.
doi:10.1016/j.bbrc.2006.02.142

encoding for tumor-associated proteins, or directly fused to or incubated with tumor cells [6]. For effective induction of cytotoxic T lymphocytes (CTLs) by vaccination, "Cross-presentation" mediated by DCs often plays an important role. Such cross-presentation includes the antigen presentation of exogenous antigens by major histocompatibility complex (MHC) class I molecules as well as by MHC class II molecules [7,8]. HSP-chaperoned peptides were cross-presented by the MHC class I molecules of the DCs several 100-fold more efficiently than unchaperoned peptides [9]. In addition, CD91, also called α_2-macroglobulin receptor is expressed on DCs and has been shown to act as one of the receptors for HSP-chaperoned peptides to efficiently incorporate the HSP–peptide complexes [10].

We earlier reported that heat shock protein 105 (HSP105) was overexpressed in a variety of human cancers but it is not expressed in normal tissue except for the testes [11,12], thus suggesting that HSP105 itself may be a potential candidate as a target antigen for cancer immunotherapy. The amino acid sequences and expression patterns of HSP105 are very similar between humans and mice. HSP105 has been found to be immunogenic in mice and an effective anti-tumor immunity has been observed after *HSP105* DNA vaccination [13]. In the present study, we set up a preclinical study to investigate the usefulness of HSP105 as a target for cancer immunotherapy using DCs. It has been reported that HSPs can induce DC maturation and activation as determined by the upregulation of MHC class II and CD86 molecules, the secretion of IL-12 and TNFα [14,15], and migration into draining lymphoid organs [16]. On the contrary, some investigators reported that HSP-mediated maturation of DCs was caused by contaminating lipopolysaccharide (LPS) fraction because endotoxin-free HSP70 failed to induce DC maturation [17]. We herein show that the highly purified HSP105 did not induce DC maturation and that the immunization of HSP105-pulsed DC led to the tumor rejection of melanoma and colorectal cancer in mice. These findings suggested that HSP105 itself could be a valuable tumor-associated antigen applicable for DC-based immunotherapy of tumors overexpressing it.

Materials and methods

Cell lines and mice. A subline of BALB/c-derived colorectal cancer cell line Colon 26, C26 (C20), was provided by Dr. Kyoichi Shimomura (Astellas Pharmaceutical Co., Tsukuba, Japan). Other cancer cell lines were kindly provided by the Cell Resource Center for Biomedical Research Institute of Development, Aging, and Cancer, Tohoku University (Sendai, Japan). All these cell lines were cultured in RPMI 1640 medium supplemented with 10% heat-inactivated fetal calf serum at 37 °C in a humidified 5% CO_2 atmosphere. We used the B16-F10 melanoma cell line syngeneic to C57BL/6 mice and C26 (C20) for the tumor challenge. Female 6- to 8-week-old C57BL/6 mice (H-2^b) and BALB/c mice (H-2^d) were purchased from Charles River Japan (Yokohama, Japan). These mice were kept under specific pathogen-free conditions. These experiments were approved by the Animal Research Committee of Kumamoto University.

Production of recombinant proteins. We produced highly purified recombinant mouse HSP105 from the *Escherichia coli* strain BL21 cells transduced with the mouse *HSP105* gene expression vector, as described previously [18]. Purified proteins were separated by sodium dodecyl sulfate–polyacrylamide gel electrophoresis (SDS–PAGE), and Coomassie brilliant blue (CBB)-stained bands were quantified by densitometry. Thereafter, by using affinity chromatography on a polymyxin B agarose gel (Sigma Chemical Co., St. Louis, MO), the endotoxin levels were decreased. We also produced highly purified recombinant myelin basic protein (MBP) as described previously [19]. Both recombinant HSP105 and MBP were estimated to be almost endotoxin free by using Limulus amebocyte lysate assay kit (BioWhittaker, Walkersville, MD), and endotoxin contents in these two materials were below 10 endotoxin U/mg.

Immunizations and tumor challenge. Bone marrow-derived DCs (BM-DC) were prepared as described previously [20]. BM-DCs were pulsed with 2 μg/ml HSP105 at 37 °C for 16 h, non-adherent and loosely adherent proliferating DCs were collected and used as HSP105-pulsed BM-DC. In tumor prevention experiments, mice were intraperitoneally inoculated with HSP105-pulsed BM-DC (5×10^5) suspended in 200 μl PBS on days −14 and −7. In parallel, groups of mice were injected with BM-DC alone or PBS as controls. Tumor challenge was initiated by subcutaneous injection with B16-F10 cells (1×10^4) or C26 (C20) cells (3×10^4) suspended in 100 μl HBSS (Gibco, Grand Island, NY) in shaved right flanks on day 0. Tumor occurrence was observed twice a week. The tumor size was evaluated by measuring two perpendicular diameters using calipers.

Flow cytometric analysis. Staining of cells and analysis on a flow cytometer (FACScan; BD Biosciences) were done as described previously [21]. Antibodies and reagents used for staining were as follows: FITC-conjugated anti-I-A^b (clone 28-16-8S; mouse IgG2a; Caltag, Burlingame, CA), R-PE-conjugated anti-mouse CD80 (clone RMMP-1; rat IgG2a; Caltag), R-PE-conjugated anti-mouse CD86 (clone RMMP-2; rat IgG2a; Caltag), FITC-conjugated anti-mouse CD4 (clone L3T4; rat IgG2a; BD PharMingen, San Diego, CA), FITC-conjugated anti-mouse CD8 (clone Ly-2; rat IgG2a; BD PharMingen), FITC-conjugated mouse IgG2a control (clone G155-178; BD PharMingen), and R-PE-conjugated rat IgG2a control (clone LO-DNP-16; Caltag).

Depletion of $CD4^+$ T cells and $CD8^+$ T cells in mice. Rat monoclonal antibodies (mAbs) GK1.5 specific to mouse CD4 and 2.43 specific to mouse CD8 were used to deplete $CD4^+$ T cells and $CD8^+$ T cells in vivo, respectively. The mice were injected with ascites (0.1 ml/mouse) from hybridoma-bearing nude mice intraperitoneally on days −18, −15, −11, −8, −4, and −1 and the tumor cells were inoculated on day 0. Normal rat IgG (Sigma, St. Louis, MO; 200 μg/mouse) was used as a control. The depletion of T cell subsets was monitored by a flow cytometric analysis, which showed more than a 90% specific depletion in the number of splenocytes.

Immunohistochemical analysis. Immunohistochemical detection of HSP105 was done as previously described [11,12]. Rabbit polyclonal anti-human HSP105 (Santa Cruz, Santa Cruz, CA) was used as the primary antibody in this study. Immunohistochemical staining of CD4 and CD8 was done as previously described [22]. For the terminal deoxynucleotidyl transferase-mediated nick end labeling (TUNEL) method, we used ApopTag Fluorescein In Situ Apoptosis Detection Kits (Serologicals Corporation, Norcross, GA).

Induction of $CD4^+$ T cells and $CD8^+$ T cells specific to HSP105. The mice were inoculated intraperitoneally with HSP105-pulsed BM-DC on days −14 and −7. Spleen cells were harvested on day 0, and $CD4^+$ T cells and $CD8^+$ T cells were purified using the magnetic cell sorting system (MACS) with anti-mouse CD4 (L3T4) mAb and anti-mouse CD8α (Ly-2) mAb, respectively. The purity of these T cell subsets exceeded 95% by a flow cytometric analysis. $CD4^+$ T cells or $CD8^+$ T cells (3×10^5/well) were separately incubated in RPMI 1640 medium supplemented with 10% horse serum, IL-2 (100 U/ml), and 2-ME (50 μM) together with the irradiated (4500 Gy) HSP105-pulsed BM-DC in 24-well culture plates. BM-DCs (3×10^4/well) pulsed with 2 μg/ml HSP105 for 16 h were irradiated (4500 Gy) and added to the culture wells for the restimulation once a week. After the third restimulation in vitro, both proliferation and cytotoxicity assays were performed as described previously [23]. For the

control of ^{51}Cr-release assay, $CD8^+$ T cells isolated from the mice immunized with BM-DCs alone were restimulated in vitro with BM-DCs alone once a week and used as effector cells.

ELISPOT assay. HSP105-specific IFN-γ production of T cells was quantified using the appropriate ELISPOT kit (BD Biosciences, San Diego, CA) according to the manufacturer's instructions. $CD4^+$ T cells or $CD8^+$ T cells were incubated with the BM-DC alone, BM-DCs pre-pulsed with HSP105, or BM-DCs pre-pulsed with myelin basic protein (MBP) as a control at 37 °C for 24 h. Each BM-DC was pre-pulsed with 2 μg/ml protein at 37 °C for 16 h. The spots were automatically counted and subsequently analyzed using the Eliphoto system (MINERVA TECH, Tokyo, Japan).

Statistical analysis. The statistical significance of the differences in the findings between the experimental groups was determined by Student's *t* test. The overall survival rate was calculated using the Kaplan–Meier method, and statistical significance was evaluated using Wilcoxon's test. A value of $P < 0.05$ was considered to be statistically significant.

Results

HSP 105 does not induce maturation of DCs

To analyze the direct effect of HSP 105 used in this study on BM-DCs, BM-DCs were incubated with HSP105, LPS as a positive control, and left untreated for 16 h. As shown in Fig. 1, no significant difference was observed in the levels of surface expression of CD80, CD86, and I-A^b between untreated BM-DCs and HSP105-pulsed BM-DCs. Moreover, HSP105-pulsed BM-DCs microscopically did not show any morphological changes in comparison to the untreated BM-DC. On the contrary, LPS-pulsed BM-DCs exhibited markedly increased expression of these three molecules. Although it is reported that HSPs could induce DC maturation and activation [14–16], the recombinant HSP105 used in this study including little LPS (below 10 endotoxin U/mg) did not show such activity. Thereafter, we evaluated the antigenicity of HSP105 to induce anti-tumor immunity.

The HSP105-pulsed BM-DC vaccine induced anti-tumor immunity against the lethal challenge of B16-F10 and C26 (C20)

We recently reported that mouse HSP105 was also overexpressed in the liver metastasis of C26 (C20) cells, and lung metastase of the B16-F10 cells, and that *HSP105* DNA vaccination inhibited the growth of these tumors [13]. In this study, we investigated the effects of HSP105 vaccination based on DCs on the growth of B16-F10 and C26 (C20) tumor cells in vivo. The objective was to determine whether prophylactic vaccination induced significant immunity against tumor growth and a prolonged survival. The protocol of vaccination in this study is shown in Fig. 2A. The results shown in Fig. 2B demonstrate that immunization with HSP105-pulsed BM-DC markedly inhibited the growth of B16-F10 tumors in comparison to other groups ($P < 0.01$). As shown in Fig. 2C, five of eight (62.5%) mice immunized with HSP105-pulsed BM-DC remained tumor free and survived for 100 days after the tumor challenge. In contrast, the mice vaccinated with BM-DC alone (12.5%) or PBS (0%) showed little protection against the growth of B16-F10 tumor in comparison to the observations in mice treated with HSP105-pulsed

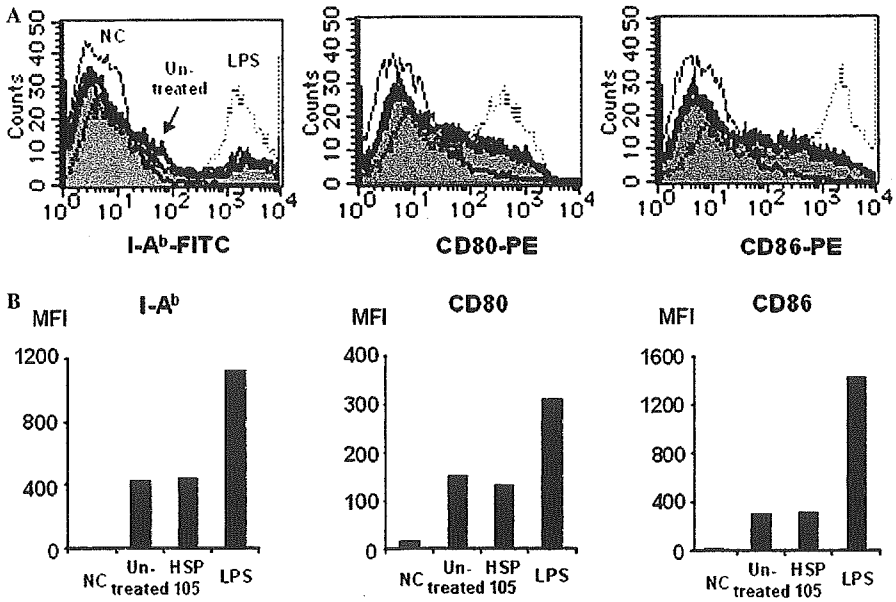

Fig. 1. Expression levels of cell surface I-A^b, CD80, and CD86 on BM-DCs, HSP105-pulsed BM-DCs, and LPS-pulsed BM-DCs were analyzed by flow cytometric analysis. BM-DCs were pulsed with 2 μg/ml HSP105, 1 μg/ml LPS or left untreated for 16 h. (A) The expression levels in HSP105-pulsed BM-DCs (filled histogram), LPS-pulsed BM-DCs (dotted line), and untreated BM-DCs (thick line), and the profiles of cells treated with isotype matched Ig as a negative control for staining (thin line). (B) The mean fluorescence intensity (MFI) of I-A^b, CD80, and CD86 staining in the cells. The results are representative of three independent experiments with similar results.

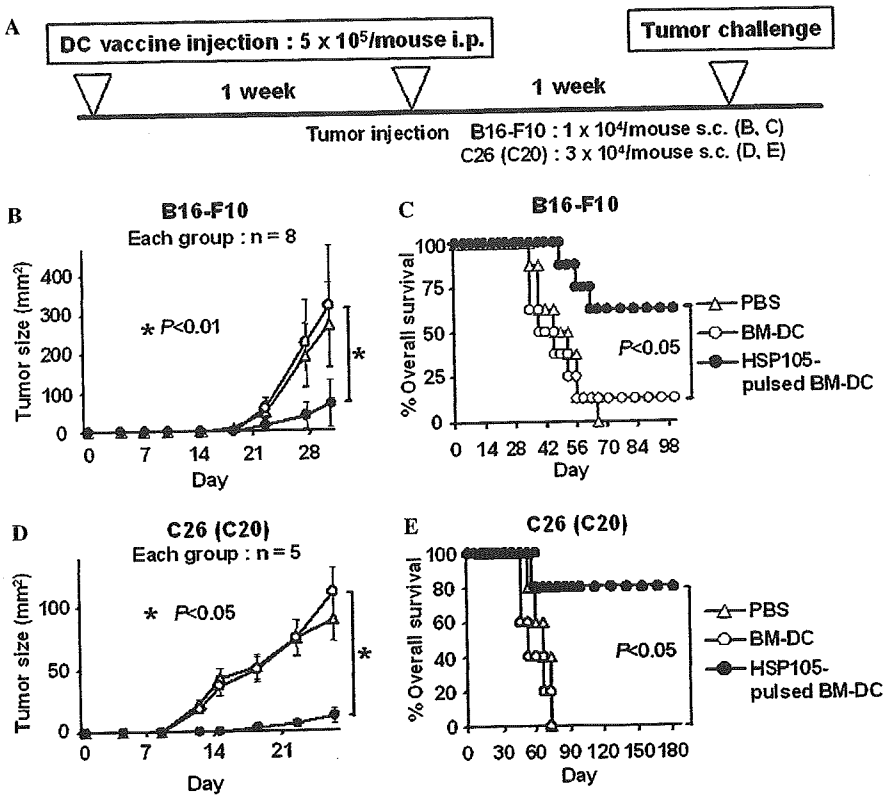

Fig. 2. Protection against tumor growth of B16-F10 and C26 (C20) cells by immunization with HSP105-pulsed BM-DC vaccine. (A) Protocol of the vaccination. The mice were immunized with PBS, BM-DC alone, and HSP105-pulsed BM-DC on 14 and 7 days before the tumor challenge. Seven days after the second immunization, the mice were challenged with B16-F10 cells s.c. (B,C), or C26 (C20) cells s.c. (D,E). (B,D) The tumor size was evaluated by measuring two perpendicular diameters. The result is presented as the mean area of tumor ± SE, and we evaluated statistical significance of the differences between each group using the unpaired Student's *t* test. (C,E) The mice in each group were observed for their survival period. The statistical significance of the differences between each group was evaluated using Wilcoxon's test.

BM-DC ($P < 0.05$). Similar results were observed in a prophylactic immunotherapy model using C26 (C20). Four of five (80%) mice immunized with HSP105-pulsed BM-DC completely rejected the C26 (C20) (3×10^4) cells (Figs. 2D and E), whereas tumors grew rapidly and all five mice died within 70 days in control mice treated with PBS or BM-DC alone. These results suggest that the HSP105-pulsed BM-DC vaccine is a potent vaccine that can efficiently induce specific anti-tumor immunity.

Both $CD4^+$ T cells and $CD8^+$ T cells are required for anti-tumor immunity

To determine the role of $CD4^+$ T cells and $CD8^+$ T cells in the protection against B16-F10 and C26 (C20) tumor cells induced by HSP105 vaccination, we depleted mice of $CD4^+$ T cells or $CD8^+$ T cells by the treatment with anti-CD4 or anti-CD8 mAb in vivo, respectively. During the depletion procedure, the mice were immunized with HSP105-pulsed BM-DC vaccine and challenged with B16-F10 or C26 (C20) cells (Fig. 3A). In both B16-F10 and C26 (C20) models, mice depleted of $CD4^+$ T cells, and $CD8^+$ T cells developed aggressively growing tumors after the challenge in comparison to the findings in control mice treated with rat IgG ($P < 0.05$) (Figs. 3B and D). The mice depleted of $CD4^+$ T cells or $CD8^+$ T cells all died by 52–65 days, whereas more than 50% of the control mice survived for 70 days ($P < 0.05$) (Figs. 3C and E). These results suggest that both $CD4^+$ T cells and $CD8^+$ T cells play crucial roles in the protective anti-tumor immunity induced by the HSP105-pulsed BM-DC vaccine.

Vaccination of HSP105-pulsed BM-DCs induced infiltrations of both $CD4^+$ T cells and $CD8^+$ T cells into tumor cells, but not into normal organs

Four of five (80%) mice immunized with the HSP105-pulsed BM-DCs completely rejected challenges of C26 (C20) cells (3×10^4) (Fig. 2E). To ascertain whether these rejections were induced by $CD4^+$ T cells or $CD8^+$ T cells, the subcutaneous inoculation of many C26 (C20) cells (1×10^6) into the right flank was done at 7 days after the second vaccination. After tumor formation, we removed the tumor and immunohistochemically stained it using anti-CD4 mAb, anti-CD8 mAb, and the TUNEL method. The infiltration of $CD4^+$ T cells and $CD8^+$ T cells into C26

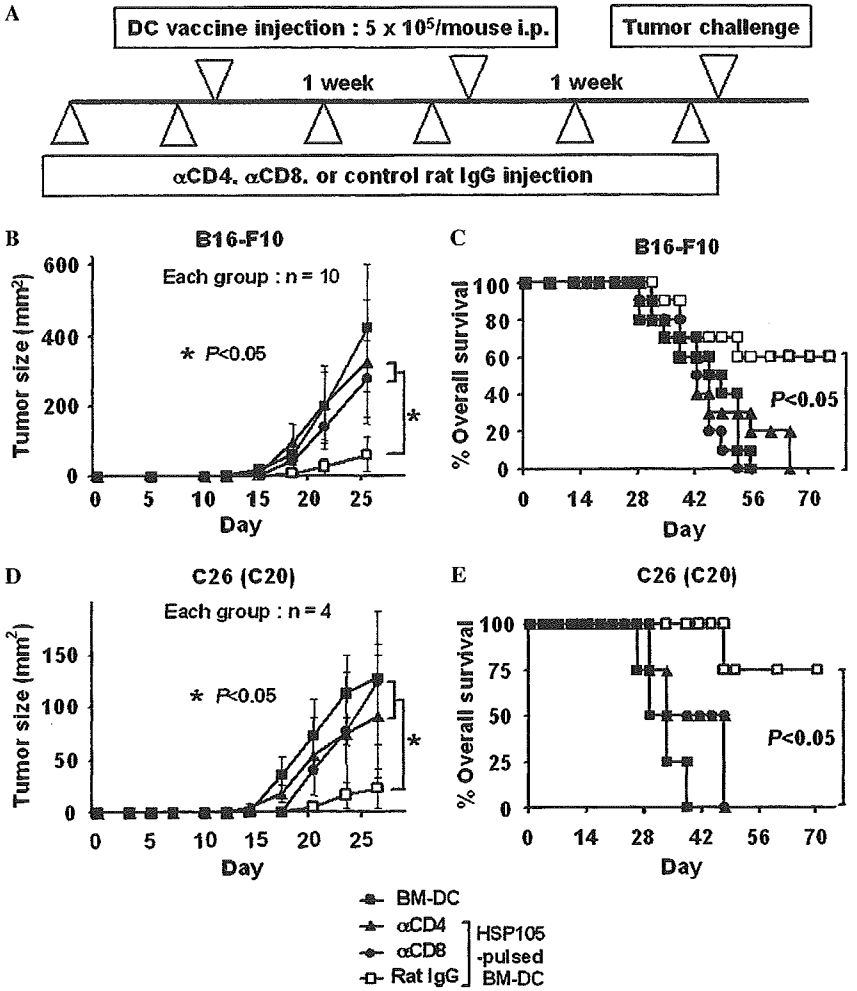

Fig. 3. Both $CD4^+$ and $CD8^+$ T cells are involved in the antitumor immunity elicited by the HSP105-pulsed DC vaccine. (A) Protocol for the vaccination and the depletion of T cells. C57BL/6 mice and BALB/c mice were challenged s.c. with B16-F10 cells and C26 (C20) cells, respectively. (B,D) The tumor size was evaluated by measuring two perpendicular diameters. The result is presented as the mean area of tumor ± SE, and we evaluated the statistical significance of the differences between each group using the unpaired Student's *t* test. (C,E) The mice in each group were observed for their survival period. The statistical significance of the differences between each group was evaluated using Wilcoxon's test.

(C20) tumors and some apoptotic C26 (C20) tumor cells were observed in the mice vaccinated with HSP105-pulsed BM-DCs, but never in the mice vaccinated with unpulsed BM-DCs (Fig. 4A). These results suggest that HSP105-pulsed BM-DCs have the potential to sensitize many HSP105-specific $CD4^+$ T cells and $CD8^+$ T cells to kill C26 (C20) tumor cells.

We evaluated the risk of autoimmunity by immunization against self-HSP105. Both BALB/c and C57BL/6 mice immunized with HSP105-pulsed BM-DC were apparently healthy without any abnormality such as dermatitis, arthritis, or neurological disorders. The tissues of the mice immunized with HSP105-pulsed BM-DC were histologically examined. The brain, liver, heart, kidneys, and spleen had normal structures and did not show any pathological changes suggestive of an immune response, such as the infiltration of $CD4^+$ T cells and $CD8^+$ T cells or tissue destruction and repair. Although we used female mice for the experiments described above, we also immunized male mice with HSP105-pulsed BM-DC to ascertain whether immunization with HSP105-pulsed BM-DC induced autoimmunity in the testis in which HSP105 is strongly expressed. However, no sign of autoimmunity was observed in the testis (Fig. 4B).

Induction of HSP105-specific $CD4^+$ T cells and $CD8^+$ T cells by immunization with HSP105-pulsed BM-DC

$CD4^+$ T cell lines specific to HSP105 were established from spleen cells derived from mice vaccinated with HSP105-pulsed BM-DC. $CD4^+$ T cells were separated from spleen cells and the purity of these cells was more than 95% by flow cytometric analysis. These cells were restimulated with irradiated and HSP105-pulsed DCs once

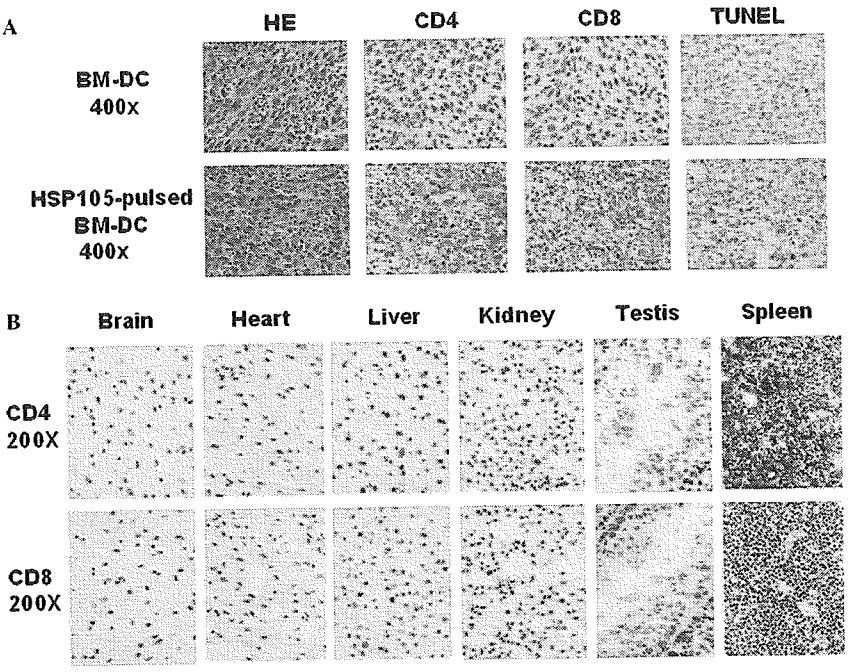

Fig. 4. Vaccination of HSP105-pulsed BM-DCs induced infiltrations of both $CD4^+$ T cells and $CD8^+$ T cells into C26 (C20) tumor and induced the apoptosis of C26 (C20) tumor cells. (A) C26 tumors removed from the mice vaccinated with BM-DCs or HSP105-pulsed BM-DCs were analyzed using immunohistochemical staining with anti-CD4 mAb, anti-CD8 mAb, and the TUNEL method on 4 days after the inoculation of tumor cells (1×10^6). (B) Normal tissue specimens of mice vaccinated with HSP105-pulsed BM-DCs were examined histologically and immunohistochemically. Objective magnification was 200×. The spleen was used as a positive control for the staining of both $CD4^+$ and $CD8^+$ cells.

a week. After three restimulations, both an ELISPOT assay and a proliferation assay were performed. The ELISPOT assay showed that HSP105-sensitized $CD4^+$ T cells produced IFN-γ in response to BM-DCs prepulsed with HSP105 but not an irrelevant MBP (Fig. 5A). As shown in Fig. 5B, HSP105-sensitized $CD4^+$ T cells proliferated in the presence of BM-DCs prepulsed with HSP105 but not MBP. These observations clearly indicated that HSP105-specific $CD4^+$ T cells were included in the T cell line.

We investigated whether HSP105-specific $CD8^+$ T cells were also induced with HSP105-pulsed DC vaccination. $CD8^+$ T cells were purified (>95%) from spleen cells of vaccinated mice and restimulated with irradiated and HSP105-pulsed DCs once a week. After three restimulations, the ELISPOT assay and 6 h ^{51}Cr-release assay were performed to detect the HSP105-specific CTL responses (Figs. 5C and D). The $CD8^+$ T cell line exhibited a HSP105-specific production of IFN-γ in an ELISPOT assay when cells were stimulated with BM-DCs prepulsed with HSP105 but not MBP ($P < 0.01$), however, the number of spots was smaller than that of $CD4^+$ T cells (Fig. 5C). $CD8^+$ T cells immunized with HSP 105-pulsed DC demonstrated a significant cytolytic activity against the B16-F10 cells pretreated with IFN-γ to induce the expression of MHC class I molecules on the cell surface, whereas $CD8^+$ T cells from mice immunized with BM-DC alone revealed little cytolytic activity ($P < 0.005$) (Fig. 5D). The induction of HSP105-specific $CD8^+$ T cells by the immunization in vivo with HSP105-pulsed BM-DC and the stimulation of the $CD8^+$ T cell line in vitro with the HSP105-pulsed BM-DC strongly suggested that these HSP105-specific $CD8^+$ T cells were induced by the cross-presentation of HSP105 by BM-DCs.

Discussion

HSPs are classified into several families based on their apparent molecular weights, such as HSP105/110, HSP90, HSP70, HSP60, HSP40, and HSP27 [24]. HSP105 consists of HSP105α and HSP105β. HSP105α is a constitutively expressed 105-kDa HSP that is induced by a variety of stresses, whereas HSP105β is a 90-kDa truncated form of HSP105α that is specifically induced by heat shock at 42 °C [24]. In this study, we used the mouse HSP105α protein. The cDNA sequence of murine HSP105 is almost the same as that of the Chinese hamster HSP110 [25,26], so HSP105 belongs to a member of the HSP105/110 family. We recently reported by the immunohistochemical analysis that HSP105 is overexpressed in a variety of human tumors [12], the liver metastasis of the C26 (C20) cells in the BALB/c mice, and lung metastasis of the B16-F10 cells in the C57BL/6 mice [13]. We examined the expression of HSP105 in the mouse cancer cell lines using a Western blotting analysis and found that HSP105 was strongly expressed in all 7 mouse cell lines tested (data not shown).

Many studies have shown that certain HSPs purified from a tumor can function as an effective vaccine against the same

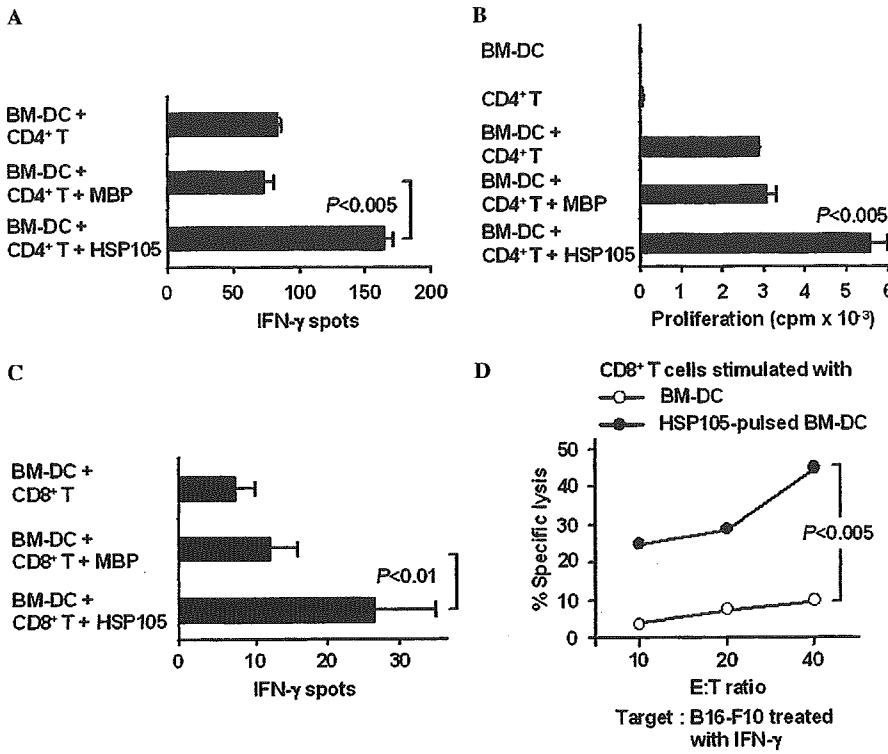

Fig. 5. Induction of HSP105-specific $CD4^+$ T cells and $CD8^+$ T cells by stimulation with HSP105-pulsed BM-DCs. (A) An ELISPOT assay for IFN-γ production by $CD4^+$ T cell lines stimulated with HSP105 protein-pulsed BM-DCs. $CD4^+$ T cells derived from the mice vaccinated with HSP105-pulsed BM-DC were stimulated in vitro with HSP105-pulsed BM-DC three times. For the ELISPOT assay, these $CD4^+$ T cells were co-cultured with BM-DC prepulsed with HSP105, MBP, or unpulsed BM-DC for 24 h. (B) Cell proliferation of $CD4^+$ T cell lines stimulated with HSP105-pulsed BM-DCs was determined by measuring [^{3}H]thymidine incorporation. $CD4^+$ T cells were co-cultured with BM-DC prepulsed with HSP105, MBP, or unpulsed BM-DC for 72 h. (C) An ELISPOT assay for IFN-γ production by $CD8^+$ T cell lines stimulated with HSP105-pulsed BM-DCs. $CD8^+$ T cells derived from mice vaccinated with HSP105-pulsed BM-DC were stimulated with HSP105-pulsed BM-DC three times in vitro. For the ELISPOT assay, these $CD8^+$ T cells were co-cultured with BM-DC prepulsed with HSP105, MBP, or unpulsed BM-DC for 24 h. (D) $CD8^+$ T cells stimulated with HSP105-pulsed BM-DC or BM-DC alone (control) were examined for their CTL activity against B16-F10 cells treated with IFN-γ (10^3 U/ml) using 6 h ^{51}Cr-release assay. The results were analyzed using the mean values of a triplicate or a quadruplicate assay. The data shown in A–D are each representative of three independent experiments with similar results.

tumor by stimulating T cells with tumor-specific peptides bound to HSPs. Subjeck and co-workers [27,28] reported that tumor-derived HSP110–peptide complexes also stimulated tumor immunity as other HSP families did in mice. Despite studies establishing a chaperoning effect of HSPs, one impediment to the full-fledged acceptance of HSPs as peptide-transporting vehicles is the lack of mass spectrometric data directly identifying HSP-associated peptides [29]. Stress-inducible proteins can be recognized by natural killer cells and CTLs as whole antigens expressed on the surface of stressed cells in humans [30]. Proteins dramatically upregulated or modified under stressful conditions should lead to increased presentation as do peptides presented by HLA class I molecules. About 25 HSP-derived peptides bound by HLA class I molecules have been identified through mass spectrometry [30]. Cancer patients have been reported to possess CTLs specific to HSP60-derived peptide [31], while HLA-A*0201-restricted HSP70-derived CTL epitopes have been identified in both an HLA-A*0201 transgenic mouse model and in humans [32]. In this study, although we did not identify HSP105-derived epitope peptides for $CD4^+$ T cells and $CD8^+$ T cells, we did prove that HSP105 itself could induce both $CD4^+$ Th-cells and $CD8^+$ CTLs specific to HSP105 as a cancer antigen. Contrary to our findings, however, Subjeck and co-workers [28] reported that HSP110 immunization did not elicit anti-tumor immunity. This discrepancy could be attributed to the difference in the methods of immunization.

It has been reported that HSPs can induce the maturation and activation of DCs as determined by upregulation of MHC class II and CD86 molecules, secretion of the IL-12 and TNFα [14,15]. However, HSP105-pulsed BM-DCs did not show any changes in comparison to the untreated BM-DC, thus suggesting that HSP105 did not induce DC maturation and activation. It is unlikely that HSP105 brought tumor-derived peptides into the culture system, because the HSP105 used in this study was the recombinant protein produced in *E. coli*. Furthermore, we recently identified HSP105-derived CTL epitopes restricted by HLA-A*0201 or -A*2402 using HLA

transgenic mouse model (unpublished data). These results also supported that HSP105 served not as a mediator for maturation of DCs, but as a cancer antigen eliciting tumor immunity.

The results of the T cell depletion study showed that the depletion of either $CD4^+$ T cells or $CD8^+$ T cells abrogated the anti-tumor immune response induced by the HSP 105-pulsed BM-DC vaccine, and that both $CD4^+$ and $CD8^+$ T cells play crucial roles in the protective anti-tumor immunity. $CD8^+$ T cells are thought to serve as the dominant effector cell mediating tumor killing, in contrast, $CD4^+$ T cells are thought to have an indirect role in providing help to CTL as well as a direct role in tumor rejection [33]. It is interesting that B16-F10 tumor cells that lack MHC class I were killed in in vivo study. We suppose that $CD4^+$ T cells may have an important role in this case. Peptides derived from HSP105 bound by MHC class II on the surface of HSP105-pulsed BM-DCs activate $CD4^+$ T cells. The activated $CD4^+$ T cells can secrete IFN-γ upon stimulation with tumor local DCs presenting tumor-derived HSP105 peptides, which contribute not only to activation of $CD8^+$ T cells but also to restoration of MHC class I expression in B16-F10 cells. The activated HSP105 specific $CD8^+$ T cells can recognize the peptides derived from HSP105 in the context of MHC class I and kill the B16-F10 cells.

In the field of cancer immunotherapy, most enthusiasm has been directed toward the use of various cancer vaccines; peptide vaccines alone, peptide plus cytokines, vaccination either with recombinant virus or with naked DNA encoding tumor antigen, and peptide pulsed on DCs [34]. DCs represent the most potent antigen presenting cells and also play an important role in the induction of specific T cell response [35]. Peptides pulsed on DCs have been reported to be the most effective vaccine in comparison to DNA vaccine or peptide–adjuvant mixture [36]. In this study, 62.5% and 80.0% of the mice immunized with HSP105-pulsed BM-DC completely rejected B16-F10 cells and C26 (C20) cells, respectively. On the other hand, only 50.0% of the mice immunized with the *HSP105*-DNA vaccine rejected these tumor cells in our previous study [13]. Although a further comparative analysis of the vaccination properties of these two strategies is required, our results suggested that protein-pulsed DCs are a more powerful vaccine than the DNA vaccine.

In this study, we used BM-DCs pulsed with HSP105 but not with HSP105-derived peptide as a cancer vaccine. We think that protein-pulsed DCs thus have an advantage over peptide-pulsed DCs. DCs are the major cell type known for its capacity to cross-present antigens [37]. In this study, HSP105-sensitized $CD8^+$ T cells responded to HSP105 in vitro by the stimulation of purified $CD8^+$ T cells with HSP105-pulsed DCs. This result strongly suggested that the HSP105-specific $CD8^+$ T cells were activated via the cross-presentation of HSP105 by BM-DCs. Although it became evident that gp96- and HSP70-chaperoned peptides can be presented to CTLs by DCs in the context of MHC class I molecules [38,39], we herein provide the first evidence that HSP itself can be cross-presented to CTLs by DCs. HSP105-pulsed DC can present peptides derived from exogenously added HSP105 in the context of not only MHC class II molecules on the surface of DCs to activate $CD4^+$ T cells, but also MHC class I molecules by cross-presentation to activate $CD8^+$ T cells. We herein showed the induction of specific $CD4^+$ T cells and $CD8^+$ T cells in vivo by stimulation with HSP105-pulsed DCs. The application of the peptide-pulsed DC as potential vaccine is limited to patients with the appropriate HLA alleles. To circumvent this limitation, we have used HSP105-pulsed DC to induce a HSP105 specific T cell response. HSP105-pulsed DCs offer the advantage of potentially presenting multiple immunogenic T cell epitopes without the need of prior knowledge of the individual patient's HLA type.

The mechanism of action of HSP105-pulsed BM-DCs injected intraperitoneally is still unclear. We think that DCs injected in the abdominal cavity might immigrate into mesenteric lymphatic vessels. Some DCs stay in mesenteric lymph nodes, others circulate in the blood via the thoracic duct and finally reach the spleen and bone marrow. Recent experimental evidence suggested that peripheral DCs migrate through the lymphatic vessels to the blood [40]. Although the present study showed that intraperitoneal injection of DCs induced an effective anti-tumor immunity in mice, comparison of effectiveness to other routes of immunization with DCs, such as intravenous, subcutaneous, and intranodal, remains to be investigated.

In conclusion, our results indicate that HSP105 itself is a tumor rejection antigen which may possibly be useful for cancer immunotherapy, and that HSP105-pulsed BM-DC vaccinations can prime HSP105-specific T cells in vivo, to prevent the subcutaneous growth of B16-F10 and C26 cancer cells expressing HSP105, without inducing autoimmune destruction. Our findings suggest that HSP105-pulsed BM-DC vaccination is a novel strategy for the prevention of cancer in patients treated surgically, who are at high risk for a recurrence of the cancer. Because of the overexpression of HSP105 in a variety of human tumors [12], clinical trial of immunotherapy targeted against HSP105 may well be applicable to various cancers.

Acknowledgments

We thank Dr. Kyoichi Shimomura (Astellas Pharmaceutical Co.) for providing the cancer cell line. This work was supported in part by Grants-in-Aid (No. 12213111 for Y. Nishmura, and No. 14770142 for T. Nakatsura) from the Ministry of Education, Science, Technology, Sports and Culture, Japan, and The Sagawa Foundation for Promotion of Cancer Research and Meiji Institute of Health Science.

References

[1] M.E. Feder, G.E. Hofmann, Heat-shock proteins, molecular chaperones, and the stress response: evolutionary and ecological physiology, Annu. Rev. Physiol. 61 (1999) 243–282.

[2] P. Srivastava, Interaction of heat shock proteins with peptides and antigen presenting cells: chaperoning of the innate and adaptive immune responses, Annu. Rev. Immunol. 20 (2002) 395–425.
[3] H. Udono, P.K. Srivastava, Heat shock protein 70-associated peptides elicit specific cancer immunity, J. Exp. Med. 178 (1993) 1391–1396.
[4] Y. Tamura, P. Peng, K. Liu, M. Daou, P.K. Srivastava, Immunotherapy of tumors with autologous tumor-derived heat shock protein preparations, Science 278 (1997) 117–120.
[5] G. Parmiani, A. Testori, M. Maio, C. Castelli, L. Rivoltini, L. Pilla, F. Belli, V. Mazzaferro, J. Coppa, R. Patuzzo, M.R. Sertoli, A. Hoos, P.K. Srivastava, M. Santinami, Heat shock proteins and their use as anticancer vaccines, Clin. Cancer Res. 10 (2004) 8142–8146.
[6] J.M. Timmerman, R. Levy, Dendritic cell vaccines for cancer immunotherapy, Annu. Rev. Med. 50 (1999) 507–529.
[7] A.J. Adler, D.W. Marsh, G.S. Yochum, J.L. Guzzo, A. Nigam, W.G. Nelson, D.M. Pardoll, $CD4^+$ T cell tolerance to parenchymal self-antigens requires presentation by bone marrow-derived antigen-presenting cells, J. Exp. Med. 187 (1998) 1555–1564.
[8] C. Kurts, W.R. Heath, F.R. Carbone, J. Allison, J.F. Miller, H. Kosaka, Constitutive class I-restricted exogenous presentation of self antigens in vivo, J. Exp. Med. 184 (1996) 923–930.
[9] F. Castellino, P.E. Boucher, K. Eichelberg, M. Mayhew, J.E. Rothman, A.N. Houghton, R.N. Germain, Receptor-mediated uptake of antigen/heat shock protein complexes results in major histocompatibility complex class I antigen presentation via two distinct processing pathways, J. Exp. Med. 191 (2000) 1957–1964.
[10] R.J. Binder, D.K. Han, P.K. Srivastava, CD91: a receptor for heat shock protein gp96, Nat. Immunol. 1 (2000) 151–155.
[11] T. Nakatsura, S. Senju, K. Yamada, T. Jotsuka, M. Ogawa, Y. Nishimura, Gene cloning of immunogenic antigens overexpressed in pancreatic cancer, Biochem. Biophys. Res. Commun. 281 (2001) 936–944.
[12] M. Kai, T. Nakatsura, H. Egami, S. Senju, Y. Nishimura, M. Ogawa, Heat shock protein 105 is overexpressed in a variety of human tumors, Oncol. Rep. 10 (2003) 1777–1782.
[13] M. Miyazaki, T. Nakatsura, K. Yokomine, S. Senju, M. Monji, S. Hosaka, H. Komori, Y. Yoshitake, Y. Motomura, M. Minohara, T. Kubo, K. Ishihara, T. Hatayama, M. Ogawa, Y. Nishimura, DNA vaccination of Hsp105 leads to tumor rejection of colorectal cancer and melanoma in mice through activation of both $CD4^+$ T cells and $CD8^+$ T cells, Cancer Sci. 96 (2005) 695–705.
[14] H. Singh-Jasuja, H.U. Scherer, N. Hilf, D. Arnold-Schild, H.G. Rammensee, R.E. Toes, H. Schild, The heat shock protein gp96 induces maturation of dendritic cells and down-regulation of its receptor, Eur. J. Immunol. 30 (2000) 2211–2215.
[15] S.B. Flohé, J. Brüggemann, S. Lendemans, M. Nikulina, G. Meierhoff, S. Flohé, H. Kolb, Human heat shock protein 60 induces maturation of dendritic cells versus a Th1-promoting phenotype, J. Immunol. 170 (2003) 2340–2348.
[16] R.J. Binder, K.M. Anderson, S. Basu, P.K. Srivastava, Heat shock protein gp96 induces maturation and migration of $CD11c^+$ cells in vivo, J. Immunol. 165 (2000) 6029–6035.
[17] H. Bausinger, D. Lipsker, U. Ziylan, S. Manié, J.P. Briand, J.P. Cazenave, S. Muller, J.F. Haeuw, C. Ravanat, H. de la Salle, D. Hanau, Endotoxin-free heat-shock protein70 fails to induce APC activation, Eur. J. Immunol. 32 (2002) 3708–3713.
[18] N. Yamagishi, H. Nishihori, K. Ishihara, K. Ohtsuka, T. Hatayama, Modulation of the chaperone activities of Hsc70/Hsp40 by Hsp105α and Hsp105β, Biochem. Biophys. Res. Commun. 272 (2000) 850–855.
[19] M. Minohara, H. Ochi, S. Matsushita, A. Irie, Y. Nishimura, J. Kira, Differences between T-cell reactivities to major myelin protein-derived peptides in opticospinal and conventional forms of multiple sclerosis and healthy controls, Tissue antigens 57 (2001) 447–456.
[20] T. Nakatsura, H. Komori, T. Kubo, Y. Yoshitake, S. Senju, T. Katagiri, Y. Furukawa, M. Ogawa, Y. Nakamura, Y. Nishimura, Mouse homologue of a novel human oncofetal antigen, Glypican-3, evokes T-cell-mediated tumor rejection without autoimmune reaction in mice, Clin. Cancer Res. 10 (2004) 8630–8640.
[21] S. Senju, S. Hirata, H. Matsuyoshi, M. Masuda, Y. Uemura, K. Araki, K. Yamamura, Y. Nishimura, Generation and genetic modification of dendritic cells derived from mouse embryonic stem cells, Blood 101 (2003) 3501–3508.
[22] H. Matsuyoshi, S. Senju, S. Hirata, Y. Yoshitake, Y. Uemura, Y. Nishimura, Enhanced priming of antigen-specific CTLs in vivo by embryonic stem cell-derived dendritic cells expressing chemokine along with antigenic protein: application to antitumor vaccination, J. Immunol. 172 (2004) 776–786.
[23] H. Fujita, S. Senju, H. Yokomizo, H. Saya, M. Ogawa, S. Matsushita, Y. Nishimura, Evidence that HLA class II-restricted human $CD4^+$ T cells specific to p53 self peptides respond to p53 proteins of both wild and mutant forms, Eur. J. Immunol. 28 (1998) 305–316.
[24] E.A. Craig, J.S. Weissman, A.L. Horwich, Heat shock proteins and molecular chaperones: mediators of protein conformation and turnover in the cell, Cell 78 (1994) 365–372.
[25] K. Yasuda, A. Nakai, T. Hatayama, K. Nagata, Cloning and expression of murine high molecular mass heat shock proteins, HSP105, J. Biol. Chem. 270 (1995) 29718–29723.
[26] D. Lee-Yoon, D. Easton, M. Murawski, R. Burd, J.R. Subjeck, Identification of a major subfamily of large hsp70-like proteins through the cloning of the mammalian 110-kDa heat shock protein, J. Biol. Chem. 270 (1995) 15725–15733.
[27] X.Y. Wang, L. Kazim, E.A. Repasky, J.R. Subjeck, Characterization of heat shock protein 110 and glucose-regulated protein 170 as cancer vaccines and the effect of fever-range hyperthermia on vaccine activity, J. Immunol. 165 (2001) 490–497.
[28] X.Y. Wang, X. Chen, M.H. Manjili, E. Repasky, R. Henderson, J.R. Subjeck, Targeted immunotherapy using reconstituted chaperone complexes of heat shock protein 110 and melanoma-associated antigen gp100, Cancer Res. 63 (2003) 2553–2560.
[29] C.V. Nicchitta, Re-evaluating the role of heat-shock protein–peptide interactions in tumour immunity, Nat. Rev. Immunol. 3 (2003) 427–432.
[30] H.D. Hickman-Miller, W.H. Hildebrand, The immune response under stress: the role of HSP-derived peptides, Trends Immunol. 25 (2004) 427–433.
[31] K. Azuma, S. Shichijo, H. Takedatsu, N. Komatsu, H. Sawamizu, K. Itoh, Heat shock cognate protein 70 encodes antigenic epitopes recognized by HLA-B4601-restricted cytotoxic T lymphocytes from cancer patients, Br. J. Cancer 89 (2003) 1079–1085.
[32] O. Faure, S. Graff-Dubois, L. Bretaudeau, L. Derré, D.A. Gross, P.M. Alves, S. Cornet, M.T. Duffour, S. Chouaib, I. Miconnet, M. Gregoire, F. Jotereau, F.A. Lemonnier, J.P. Abastado, K. Kosmatopoulos, Inducible HSP70 as target of anticancer immunotherapy: identification of HLA-A*0201-restricted epitopes, Int. J. Cancer 108 (2004) 863–870.
[33] K. Hung, R. Hayashi, A. Lafond-Walker, C. Lowenstein, D. Pardoll, H. Levitsky, The central role of $CD4^+$ T cells in the antitumor immune response, J. Exp. Med. 188 (1998) 2357–2368.
[34] S.A. Rosenberg, J.C. Yang, N.P. Restifo, Cancer immunotherapy: moving beyond current vaccines, Nat. Med. 10 (2004) 909–915.
[35] J. Banchereau, R.M. Steinman, Dendritic cells and the control of immunity, Nature 392 (1998) 245–252.
[36] M. Bellone, D. Cantarella, P. Castiglioni, M.C. Crosti, A. Ronchetti, M. Moro, M.P. Garancini, G. Casorati, P. Dellabona, Relevance of the tumor antigen in the validation of three vaccination strategies for melanoma, J. Immunol. 165 (2000) 2651–2656.
[37] M.L. Albert, B. Sauter, N. Bhardwaj, Dendritic cells acquire antigen from apoptotic cells and induce class I-restricted CTLs, Nature 392 (1998) 86–89.
[38] E. Noessner, R. Gastpar, V. Milani, A. Brandl, P.J. Hutzler, M.C. Kuppner, M. Roos, E. Kremmer, A. Asea, S.K. Calderwood, R.D. Issels, Tumor-derived heat shock protein 70 peptide complexes are cross-presented by human dendritic cells, J. Immunol. 169 (2002) 5424–5432.

[39] H. Singh-Jasuja, R.E. Toes, P. Spee, C. Münz, N. Hilf, S.P. Schoenberger, P. Ricciardi-Castagnoli, J. Neefjes, H.G. Rammensee, D. Arnold-Schild, H. Schild, Cross-presentation of glycoprotein 96-associated antigens on major histocompatibility complex class I molecules requires receptor-mediated endocytosis, J. Exp. Med. 191 (2000) 1965–1974.

[40] L.L. Cavanagh, R. Bonasio, I.B. Mazo, C. Halin, G. Cheng, A.W. van der Velden, A. Cariappa, C. Chase, P. Russell, M.N. Starnbach, P.A. Koni, S. Pillai, W. Weninger, U.H. von Andrian, Activating of bone marrow-resident memory T cells by circulating, antigen-bearing dendritic cells, Nat. Immunol. 6 (2005) 1029–1037.

Molecular Microbiology (2006) 59(1), 99–112

doi:10.1111/j.1365-2958.2005.04938.x
First published online 27 October 2005

Release of the type I secreted α-haemolysin via outer membrane vesicles from *Escherichia coli*

Carlos Balsalobre,[1*†] Jose Manuel Silván,[1] Stina Berglund,[1] Yoshimitsu Mizunoe,[2] Bernt Eric Uhlin[1] and Sun Nyunt Wai[1]

[1]*Department of Molecular Biology, Umeå University, S-90187 Umeå, Sweden.*

[2]*Department of Bacteriology, Faculty of Medical Sciences, Kyushu University, Fukuoka 812–8582, Japan.*

Summary

The α-haemolysin is an important virulence factor commonly expressed by extraintestinal pathogenic *Escherichia coli*. The secretion of the α-haemolysin is mediated by the type I secretion system and the toxin reaches the extracellular space without the formation of periplasmic intermediates presumably in a soluble form. Surprisingly, we found that a fraction of this type I secreted protein is located within outer membrane vesicles (OMVs) that are released by the bacteria. The α-haemolysin appeared very tightly associated with the OMVs as judged by dissociation assays and proteinase susceptibility tests. The α-haemolysin in OMVs was cytotoxically active and caused lysis of red blood cells. The OMVs containing the α-haemolysin were distinct from the OMVs not containing α-haemolysin, showing a lower density. Furthermore, they differed in protein composition and one component of the type I secretion system, the TolC protein, was found in the lower density vesicles. Studies of natural isolates of *E. coli* demonstrated that the localization of α-haemolysin in OMVs is a common feature among haemolytic strains. We propose an alternative pathway for the transport of the type I secreted α-haemolysin from the bacteria to the host cells during bacterial infections.

Introduction

The different protein secretion systems currently described for Gram-negative bacteria establish how secreted proteins are transported through the bacterial envelopes to the extracellular milieu, where the proteins presumably then will diffuse in a soluble form to contact the target molecules or tissues. However, recent studies have shown that transport of secreted proteins to the extracellular space may involve high-order complexes with lipid membranes structures, the outer membrane vesicles (OMVs) (Wai *et al.*, 2003). From the surface of Gram-negative bacteria there is a constant formation of OMVs, presumably as a consequence of normal bacterial growth and metabolism (Beveridge, 1999). Although the mechanism of OMVs biogenesis is not fully understood, it has been proposed that they may play a role in protein export, virulence by mediating bacterial adherence to host cells, transfer of DNA between different bacterial cells and evasion of the immune system (Shoberg and Thomas, 1993; Wai *et al.*, 1995; Kolling and Matthews, 1999; Saunders *et al.*, 1999; Horstman and Kuehn, 2002; Wai *et al.*, 2003). When OMVs are formed, the different periplasmic proteins are more or less efficiently included as luminal cargo (Kadurugamuwa and Beveridge, 1995; Horstman and Kuehn, 2000; Wai *et al.*, 2003).

Secretion by the type I secretion system involves the direct transfer of the proteins from the cytoplasm to the extracellular space without the formation of periplasmic intermediates through a contiguous protein transmembrane channel generated by the type I secretion apparatus (Felmlee and Welch, 1988; Thanabalu *et al.*, 1998). Therefore, the secretion of proteins by the type I secretion system *per se* does not require any direct interaction between the secreted protein and the cell membranes. The α-haemolysin from *Escherichia coli* is an exotoxin frequently associated with strains isolated from extraintestinal infections such as uropathogenic *E. coli* (UPEC) and it is one of the best characterized examples of bacterial proteins that are secreted by the type I secretion system. The α-haemolysin belongs to the family of RTX toxins that include several bacterial proteins with conserved protein features and common genetic organization. The synthesis, activation and secretion of the α-haemolysin are determined by the *hlyCABD* operon (Welch, 1991). The α-haemolysin is synthesized in an inactive form with a molecular weight of 110 kDa, which is activated in the cytoplasm to the haemolytically active form by HlyC, a fatty acid acyltransferase (Stanley *et al.*, 1998). The α-haemolysin is directly secreted from the cytoplasm to the extracellular space through a transmem-

Accepted 28 September, 2005. *For correspondence. E-mail cbalsalobre@ub.edu; Tel. (+34) 93 402 1492; Fax (+34) 93 403 4629. †Present address: Departament de Microbiologia, Facultat de Biologia, Universitat de Barcelona, Avgda Diagonal, 645. 08028 Barcelona, Spain.

brane channel consisting of HlyB, HlyD and TolC (Thanabalu *et al.*, 1998). The inner membrane proteins HlyB and HlyD are specific components of the transport apparatus of the α-haemolysin whereas TolC is a multifunctional protein located in the outer membrane of *E. coli* (Wandersman and Delepelaire, 1990; Thanabalu *et al.*, 1998; Koronakis, 2003). The secreted α-haemolysin has cytolytic and/or cytotoxic activity against a wide range of mammalian cell types (Lally *et al.*, 1999).

Interestingly, it has been described that a fraction of the secreted α-haemolysin from *E. coli* remains located on the bacterial cell surface (Oropeza-Wekerle *et al.*, 1989). In this work, we describe experiments aimed at determining the location of the α-haemolysin when it is secreted from *E. coli* cells. Remarkably, our findings demonstrate that a considerable portion of this type I secreted α-haemolysin is associated with OMVs and that it is present there in a physiologically active form. We suggest that OMVs may play an important role in the transport/dissemination of the α-haemolysin to the host cells tissue during bacterial infections.

Results

A fraction of the secreted α-haemolysin is associated with bacterial vesicles

To further localize the α-haemolysin upon secretion we decided to investigate whether the secreted α-haemolysin was associated with vesicles. The vesicles from cultures of the α-haemolysin producing strain MC1061/pANN202-312R and the strain MC1061/pACYC184 (vector control) were isolated and analysed by electrophoresis. The isolation procedure includes removing bacterial cells by filtration of the culture supernatant and an ultracentrifugation step to collect vesicles from the cell-free culture supernatant (see *Experimental procedures* for details). The results (Fig. 1A) revealed a major band of an estimated molecular weight of 110 kDa detected in the vesicles isolated from MC1061/pANN202-312R, corresponding presumably to the α-haemolysin. That band was also detected in the whole cell extract from the same strain. Furthermore, there was no such band detected neither in the vesicles nor in the whole cell extract from the control strain. By immunoblot analysis with specific polyclonal anti α-haemolysin antiserum, we confirmed that the detected band represented the α-haemolysin (Fig. 1B). Ultrastructural analysis of vesicles was performed by electron microscopy (EM). The vesicles produced by the strain MC1061/pACYC184 were homogeneous in both size (average diameter of 50 nm) and morphology (Fig. 1C). On the other hand, the vesicles produced by the strain MC1061/pANN202-312R, which expressed the α-haemolysin, were heterogeneous (Fig. 1D). Two different subpopulations of vesicles were detected: (i) smaller vesicles that resemble in size and morphology those observed in the samples of MC1061/pACYC184; and (ii) larger vesicles (average diameter of 150 nm) with a thinner margin, indicated with arrows in Fig. 1D. Taken together, these results suggest that the secreted α-haemolysin is present not only as a soluble secreted form, but also associated with vesicles. In order to study the relevance of this finding in relation to the current model of secretion and transport of the α-haemolysin we considered that it would be of interest to estimate what percentage of the secreted α-haemolysin was vesicle-associated. To test this, the amount of (i) total secreted α-haemolysin in cell-free supernatants (before isolation of vesicles); (ii) soluble α-haemolysin (cell-free supernatant after removal of the vesicles by centrifugation); and (iii) vesicle-associated α-haemolysin (vesicles collected by centrifugation) were determined for three independent cultures of the strain MC1061/pANN202-312R. For each culture the amount of total secreted α-haemolysin was given arbitrarily the value of 100. The results, given as a percentage, indicated that most of the secreted α-haemolysin was

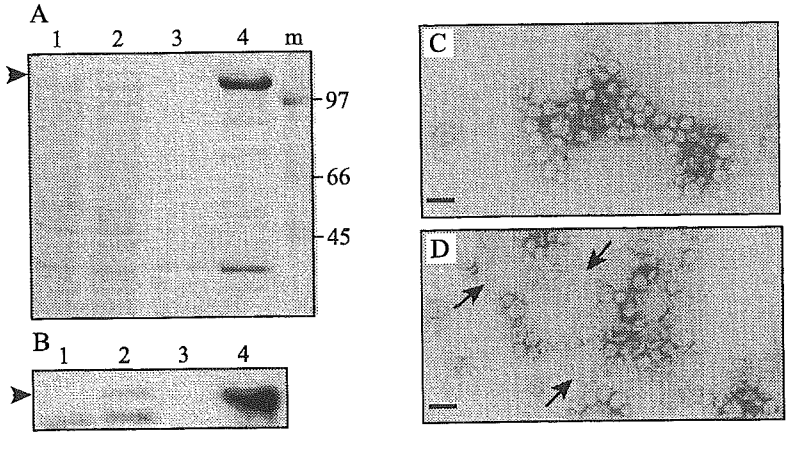

Fig. 1. The α-haemolysin is present in vesicles.
A. Electrophoretical analysis of whole cell extract (lanes 1, 2) and vesicles (lanes 3, 4) of MC1061/pACYC184 (lanes 1, 3) and MC1061/pANN202-312R (lanes 2, 4) cultures. Coomassie blue stained 10% SDS-PAGE. Lane m: molecular mass markers (size in kDa indicated along the right side). The band corresponding to the α-haemolysin is indicated with an arrowhead.
B. Immunoblot analysis of the same samples as in A using anti-α-haemolysin antibodies.
C and D. Electron micrographs of MC1061/pACYC184 (C) and MC1061/pANN202-312R (D) vesicles, bar equal to 100 nm.

associated with vesicles (66 ± 6%), whereas a smaller fraction was present in a free soluble form in the supernatant (34 ± 6%).

The α-haemolysin is tightly associated to vesicles

The above results could indicate that either the α-haemolysin was physically associated with the vesicles or alternatively that the α-haemolysin copurified together with the vesicles. To distinguish between the two possibilities dissociation assays were performed (Fig. 2A). Treatment of the vesicles with high salt concentration (either 1 M NaCl or 0.1 M Na_2CO_3) did not extract the α-haemolysin from the vesicles to any greater extent than that observed with HEPES buffer alone. Treatment with urea (0.8 M) did not affect the vesicle association of the α-haemolysin (Fig. 2A). Moreover, dissociation assays with increasing concentrations of urea (1.5 and 8 M) showed that the interaction of the α-haemolysin with the vesicles was highly resistant to the urea treatment (Fig. S1, *Supplementary material*). We conclude that protein aggregation could not be the reason for the presence of the α-haemolysin in the vesicle preparation. However, treatment with non-ionic detergent (0.5% Triton X-100) liberated all the α-haemolysin to the supernatant as a result of the vesicle membrane disruption. Control experiments using soluble α-haemolysin did rule out the possibility that the α-haemolysin simply precipitated in presence of the high

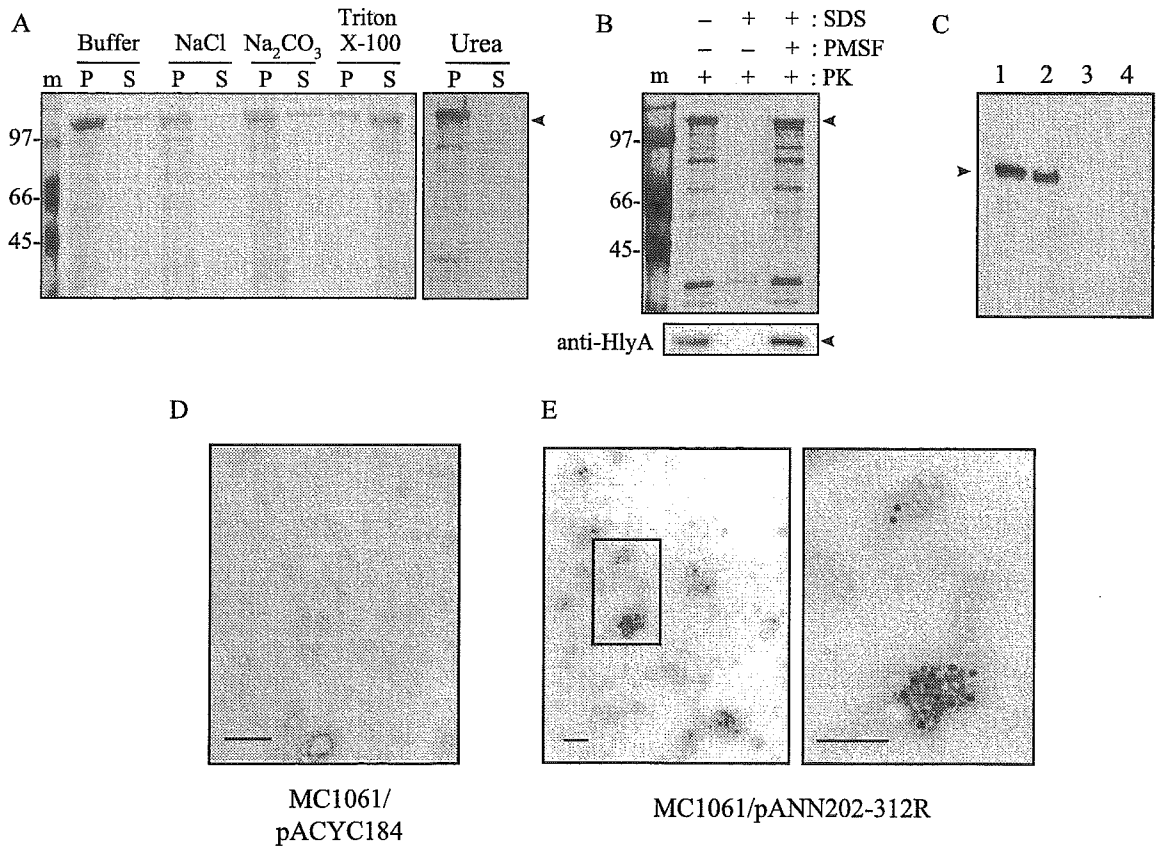

Fig. 2. The α-haemolysin is tightly associated with the vesicles.
A. Dissociation assays using vesicles from MC1061/pANN202-312R. Samples of vesicles in 20 mM Tris HCl pH 8.0 were treated for 60 min on ice in presence of: 20 mM Tris HCl pH 8.0 (buffer) or NaCl (1 M) or Na_2CO_3 (0.1 M) or Urea (0.8 M) or TritonX-100 (0.5%) respectively. The samples were then centrifuged and the resulting pellets (P) and supernatants (S) were analysed by 10% SDS-PAGE and Silver stained.
B. Proteinase K susceptibility assay. Equal amounts of vesicles from MC1061/pANN202-312R were treated with 0.5 μg ml^{-1} of proteinase K (PK). When indicated 1% SDS and 1 mM PMSF, a proteinase K inhibitor, were added. Samples were analysed in 10% SDS-PAGE and either silver stained (upper panel) or subjected to immunoblot analysis using polyclonal anti-α-haemolysin serum (bottom panel). In A and B lane m corresponds to the molecular mass markers (size in kDa indicated along the left side).
C. Immunoblot analysis using the monoclonal anti-α-haemolysin antibody E2 of the whole cell extract (lanes 1 and 3) and vesicles preparations (lanes 2 and 4) of cultures of the strains MC1061/pANN202-312R (lanes 1 and 2) and MC1061/pACYC184 (lanes 2 and 4). In A–C the band corresponding to the α-haemolysin is indicated with an arrowhead.
D–E. Immunogold-labelling (10 nm diameter gold particles) of HlyA using the monoclonal antibody E2 and vesicle preparations isolated from the strains MC1061/pACYC184 (Fig. 2D) and MC1061/pANN202-312R (Fig. 2E). The right panel in Fig. 2E is an enlargement of the indicated area in the left panel. Bars; 100 nm.

concentration of salts and thereby was recovered together with the vesicles (data not shown). Therefore, we conclude that the α-haemolysin was associated tightly with the vesicles and only when the membrane structure was disrupted did the toxin appear in soluble form. Proteinase K protection assays supported the above results. As shown in Fig. 2B, when vesicles from MC1061/pANN202-312R were incubated with Proteinase K in presence or absence of SDS, proteolytic digestion of the α-haemolysin was detected in presence of detergent (1% SDS) but no, or very little, digestion occurred in absence of the membrane disrupting agents, indicating that the α-haemolysin was partially protected by the vesicle structure. Control experiments using soluble α-haemolysin showed that the protein was proteinase K-sensitive both in presence or absence of the detergent.

In order to test if free α-haemolysin might readily attach to OMVs, experiments were performed where purified α-haemolysin was mixed with OMVs from a non-haemolytic strain (MC1061/pACYC184). However, no spontaneous association of the soluble α-haemolysin with the OMVs from MC1061/pACYC184 was detected (data not shown).

Electron microscopy analyses by immunogold-labelling of HlyA in vesicle preparations from the strains MC1061/pACYC184 and MC1061/pANN202-312R were performed using an anti-HlyA monoclonal antibody. As shown by Western blot, the antibody specifically recognized the α-haemolysin in both total cell extract and vesicle preparations from the strain MC1061/pANN202-312R and did not cross-react with proteins from the control strain MC1061/pACYC184 (Fig. 2C). Furthermore, in the EM analyses a positive gold labelling was only detected in case of the vesicle preparations from strain MC1061/pANN202-312R (Fig. 2D and E). Interestingly, no gold deposition was found in areas with intact vesicles but intense deposition of gold particles was detected only in areas where vesicles structures seemed disrupted. (Fig. 2E).

The vesicles produced by haemolytic strains are OMVs

Presumably different kinds of vesicles could in principle be produced by Gram-negative bacteria: vesicles containing both outer and inner membranes and vesicles containing only either type of membrane. To determine the nature of the vesicles from the strain MC1061/pANN202-312R we monitored the presence of specific protein markers for the outer membrane, inner membrane and the cytosol (Fig. 3). The presence of two outer membrane proteins, OmpA and TolC, was detected using specific polyclonal antibodies in both whole cell extract and vesicles from MC1061/pANN202-312R. To detect the presence of inner membrane in vesicle preparations, the NADH oxidase activity, a well established inner membrane marker was determined. As controls, both outer and inner membranes

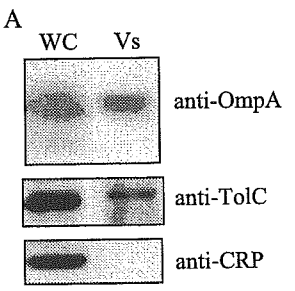

B

NADH oxydase activity (mM/min x μg protein)	
IM	1.21
OM	0.21
Vs	0.018

Fig. 3. Composition of the vesicles produced by MC1061/pANN202-312R.
A. Immunoblot analyses of both whole cells extract (WC) and vesicles preparations (Vs) from cultures of MC1061/pANN202-312R using the specific antisera indicated. WC was loaded the equivalent to 75 μl of a culture with an OD_{600} of 0.8; Vs was loaded the vesicles recovered from 4 ml of a culture with an OD_{600} of 0.8.
B. NADH oxidase- specific activity of inner membrane (IM), outer membrane (OM) and vesicle (Vs) preparations of MC1061/pANN202-312R.

were isolated from MC1061/pANN202-312R. The specific NADH oxidase activity detected in vesicle preparations was very low when compared with the inner membrane fractions. Furthermore, immunoblotting indicated that the cytoplasmic protein CRP was absent from the vesicles. These results strongly indicated the absence of inner membrane in the vesicles and we conclude that the vesicles from α-haemolysin-producing *E. coli* were OMVs.

The α-haemolysin associated with OMVs is active

To investigate if the α-haemolysin associated with OMVs was active we tested it in different assays. The cytolytic activity against red blood cells was tested by measuring the release of haemoglobin after co-incubation of horse blood with OMVs from both MC1061/pACYC184 and MC1061/pANN202-312R strains. The results (Fig. 4A) provided clear evidence for cytolytic activity associated with the OMVs from MC1061/pANN202-312R but there was little or no such activity in the OMVs from MC1061/pACYC184. Furthermore, virtually no haemoglobin release was detected in absence of calcium, which is consistent with the fact that the activity of the α-haemolysin is calcium-dependent. The activity of the α-haemolysin associated with OMVs was also tested on nucleated cells by monitoring the induction of cell detachment using HeLa cells monolayers. When testing either the bacterial cultures or the cell-free supernatants (including OMVs) from the strain MC1061/pANN202-312R we observed massive loss of the HeLa cell monolayer, more than 50% of the cells were detached after 90 min (Fig. 4B). A similar level of cell monolayer disruption was observed when OMVs from the α-haemolysin producing bacteria were tested. In contrast, no disturbance of the HeLa cell monolayer was observed when samples of the negative control

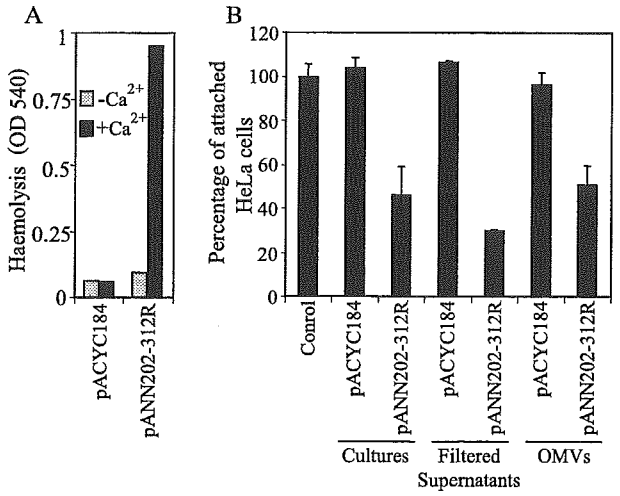

Fig. 4. The α-haemolysin present in OMVs is active.
A. Haemolytic activity of OMVs isolated from cultures of MC1061/pACYC184 and MC1061/pANN202-312R in either the absence (grey bars) or the presence (black bars) of 10 mM $CaCl_2$.
B. HeLa cell monolayer detachment activity. Percentage of remaining attached HeLa cells, measured as OD_{590}, after 90 min incubation in presence of either bacterial culture or filtered supernatant or OMVs preparation from strains MC1061/pACYC184 and MC1061/pANN202-312R. The results are the average of three independent experiments. For each experiment the OD_{590} after incubation in presence of buffer (control) was given arbitrarily the value 100. The error bars indicate the standard deviation among the experiments.

strain MC1061/pACYC184 were tested. Taken together, these results confirm that the α-haemolysin present in OMVs was active in both lytic (on red blood cells) and non-lytic (on HeLa cells) assay systems.

The localization of the α-haemolysin in OMVs is independent of the HlyC-mediated fatty acid acylation

The activity of the α-haemolysin is strictly dependent of a fatty acid acylation catalysed by HlyC in the cytoplasm. Previously, it has been described that the acylation is not required for the secretion of the α-haemolysin (Stanley *et al.*, 1998). To find out whether the localization of the α-haemolysin in OMVs requires this post-translational modification, OMVs from strains W3110/pANN202-812 (*hlyA*$^+$*hlyC*$^+$), W3110/pANN202-812B (*hlyA*$^+$*hlyC*) and W3110/pBR322 (vector control) were isolated and analysed both electrophoretically and by EM. The results (Fig. 5A) indicated that both the acylated α-haemolysin and the non-acylated α-haemolysin were present in the OMVs. EM analysis showed that OMVs containing the non-acylated α-haemolysin (from strain W3110/pANN202-812B, *hlyA*$^+$*hlyC*) appeared identical to the OMVs containing acylated α-haemolysin (Figs 5B and 1D). We here show results obtained with the *E. coli* K-12 strain W3110 background. The results with strain MC1061/pANN202-812B were completely consistent (data not shown). This comparison also thereby verified that the findings on HlyA in OMVs obtained with the MC1061 derivatives were not a strain-specific phenomenon. We conclude that the association of the α-haemolysin to OMVs is independent of the HlyC-mediated fatty acid acylation.

It was earlier shown that haemolysin is, after synthesis, rapidly detected in culture supernatants (Felmlee and Welch, 1988). To study the kinetics of the localization of newly synthesized α-haemolysin in OMVs, proteins were labelled by a 20 s pulse of radiolabelled methionine and soluble and OMVs fractions from supernatants of MC1061/pANN202-312R cultures were analysed (see *Experimental procedures* for details). Newly synthesized α-haemolysin was appearing within 20 s labelling period in both fractions: OMVs and soluble (Fig. 6). The result shown is fully consistent with the data on the kinetics of total secreted α-haemolysin previously published (Felmlee and Welch, 1988) and suggests a very quick association of the newly synthesized α-haemolysin with the OMVs. Furthermore, a quantification of the radiolabelled α-haemolysin in OMVs and in the soluble form showed that a great majority (> 90%) of the newly synthesized α-haemolysin was associated with the OMVs and thereby the result was consistent with previous estimations.

A particular feature of the secretion of the α-haemolysin is that it is dependent on a domain located in the carboxy terminal domain of the protein. It is known that the 23 kDa carboxy terminal domain of the α-haemolysin is sufficient for the export through the membranes (Nicaud *et al.*, 1986). Experiments with an epitope-tagged construct

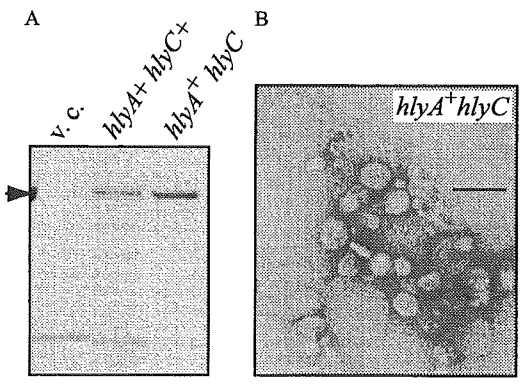

Fig. 5. The localization of the α-haemolysin in OMVs is independent of the HlyC-mediated acylation.
A. Electrophoretical analysis (Coomassie stained 10% SDS-PAGE) of the OMVs preparations of the strains W3110/pBR322 (vector control, v.c), W3110/pANN202-812 (*hlyA*$^+$ *hlyC*$^+$) and W3110/pANN202-812B (*hlyA*$^+$ *hlyC*). The band corresponding to the α-haemolysin is indicated by an arrowhead.
B. Electron micrographs of W3110/pANN202-812B OMVs. Bar; 100 nm.

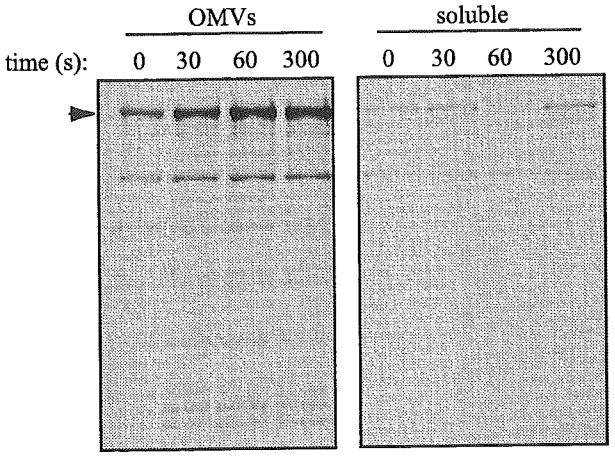

Fig. 6. The localization of the α-haemolysin in OMVs is very fast after synthesis and secretion. Electrophoretical analysis (10% SDS-PAGE) of the OMVs and soluble fractions of the supernatant of cultures of the strain MC1061/pANN202-312R after [^{35}S]Methionine was incorporated for 20 s. The length of the chase period is indicated at the top in seconds. The band that was identified by immunoblot as the α-haemolysin (data not shown) is indicated with an arrowhead.

of the 23 kDa C-terminal secretion signal of the α-haemolysin (Fernandez *et al.*, 2000) were performed to investigate whether the carboxy terminal domain itself also could determine the localization of the α-haemolysin in the OMVs. The results obtained indicated that this domain, which is essential for its secretion, is not sufficient for its localization in the OMVs (Fig. S2, *Supplementary material*).

Altered protein composition and morphology of α-haemolysin containing OMVs

The presence of a fraction of larger OMVs in the preparations of MC1061/pANN202-3012R but not in MC1061/pACYC184 (Fig. 1) led us to hypothesize that the larger OMVs harboured the α-haemolysin. To test this hypothesis, the OMVs from MC1061/pANN202-312R were fractionated in a density gradient and the fractions obtained were analysed for the protein composition (Fig. 7A). The protein bands corresponding to OmpA and the α-haemolysin were identified by Western blotting (data not shown) and the relative content of these proteins in the different fractions was quantified and plotted (Fig. 7B). The gradient profile of OmpA indicated the existence of two populations of OMVs with different density that peaked in fractions No. 9 and No. 15 respectively. The detection of lipopolysaccharide (LPS) by silver staining after SDS-PAGE analysis of the different Optiprep gradient fractions also suggested that OMVs were distributed in the density gradient as two peaks around fractions No. 9 and No. 15 respectively (data not shown). Interestingly, most of the α-haemolysin (> 70%) was present in the same fractions as the low-density OMVs (fractions 9–10). When the calcium-dependent cytolytic activity against red blood cells was monitored (Fig. 7C), the maximal activity was detected, as expected, in case of the fractions containing the α-haemolysin-enriched OMVs. Notably, the TolC protein, the outer-membrane component of the type I secretion machinery, was only detected in the fractions containing the majority of the α-haemolysin. In fact, more than 95% of the total TolC was found in the fractions No. 9 and No. 10 by immunoblot analysis (Fig. 7D). The absence of detectable TolC in the fractions No. 14 and No. 15, which contained similar amounts of OmpA protein, indicates a differential protein composition of the OMVs containing α-haemolysin versus the OMVs not containing α-haemolysin. Silver staining analyses of the protein content of the fractions No. 9 and No. 15 revealed additional differences in the protein composition (Fig. 7E). Similar protein profiles as that of fractions No. 9 and No. 15 were observed in the case of fractions No. 10 and No. 14 respectively (data not shown). Thin-layer chromatography (TLC) studies indicated that the phospholipids composition was not altered in the OMVs of strains producing α-haemolysin when compared with the control strain. Furthermore, no significant differences in the phospholipids composition were detected between the two population of OMVs separated by fractionation in a density gradient, fractions No. 9 and No. 15 (Fig. S3, *Supplementary material*).

Electron microscopy analyses were performed on fractions No. 9 and No. 15 as well as on the OMVs sample used for the vesicle fractionation (input). As shown in Fig. 7F the vesicle preparation from MC1061/pANN202-312R (input) contained two clearly different subpopulations of OMVs (see also Fig. 1D). In the fraction No. 9 we observed a clear enrichment of the larger OMVs with thinner margin that were only detected in preparations from strains producing α-haemolysin. By using the difference in size among OMVs, we could estimate that in the input the amount of large OMVs (> 150 nm) was approximately 4% ($n = 1200$), although in the fraction No. 9 it was approximately 25% ($n = 190$). Moreover, most of small OMVs (< 150 nm) observed in the fraction No. 9 had the thinner margin like that observed in case of the large OMVs and different from the appearance of the margin of the OMVs recovered in fraction No. 15. Furthermore, most of the OMVs present in the fraction No. 15 resembled the vesicles that were detected in OMVs preparations from the control strain. As most of the α-haemolysin and the haemolytic activity were detected in fraction No. 9 we concluded that these low density vesicles are the ones containing the α-haemolysin. When OMVs from the strain MC1061/pACYC184 (vector control) were fractionated in an

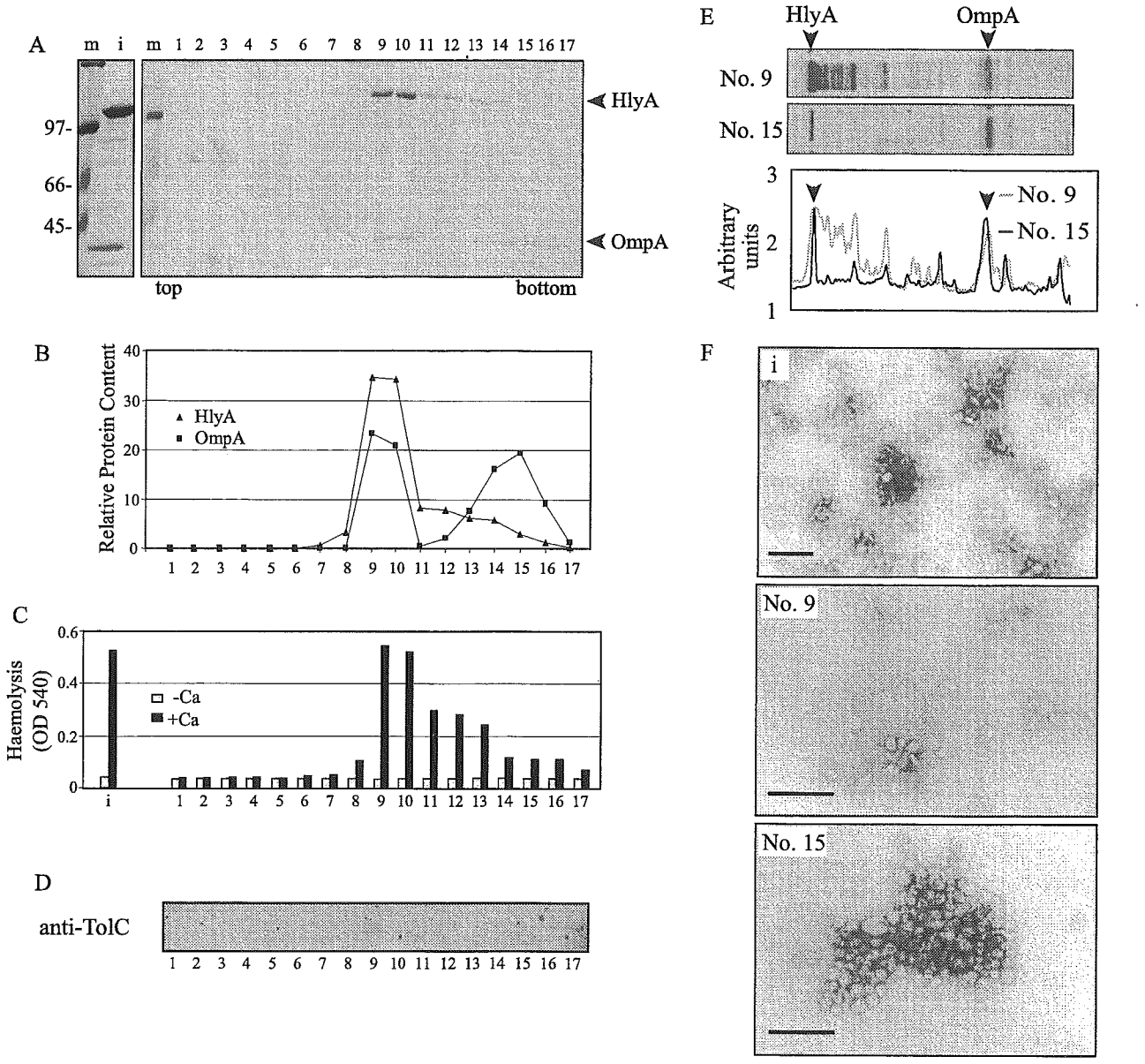

Fig. 7. Density gradient fractionation of OMVs from MC1061/pANN202-312R.
A. Electrophoretical analysis (Coomassie stained 10% SDS-PAGE) of the density gradient fractions from top (No. 1, lowest density) to bottom (No. 17, highest density) from MC1061/pANN202-312R OMVs. The bands corresponding to the α-haemolysin and OmpA are indicated. Lane m, molecular mass markers (size in kDa indicated along the left side); lane i, input OMVs from MC1061/pANN202-312R.
B. The quantification of the amounts of α-haemolysin (triangles) and OmpA (squares) in the different fractions was performed by densitometry and plotted on a relative scale.
C. Haemolytic activity of the gradients fractions from A either in presence (black bars) or in absence (grey bars) of calcium. The haemolytic activity of the input is shown by the leftmost columns (i).
D. Immunoblot analysis of the different fractions using anti-TolC serum.
E. Silver staining analysis after 10% SDS-PAGE of the proteins present in fractions No. 9 and No. 15. A densitometric analysis of the silver stained protein bands is shown in the lower panel. The bands corresponding to the α-haemolysin and OmpA are indicated by vertical arrowheads.
F. Electron micrographs of OMVs from MC1061/pANN202-312R (i: Input); fractions No. 9 and No. 15. Bar equal to 250 nm.

Optiprep gradient and OmpA was detected, a uniform population of OMVs was observed, which migrated through the gradient in a manner similar to that of the fractions No. 14–15 from the MC1061/pANN202-312-R OMVs preparations (data not shown).

Localization of secreted α-haemolysin in OMVs from different E. coli *isolates*

To determine if the transport of the α-haemolysin by OMVs was a common feature in haemolytic *E. coli* strains

we used four different isolates from both human and animal hosts, the strains ER52, ER53, ER54 and ER60. These strains belong to the B2 subgroup (typical of extraintestinal *E. coli*) of the *E. coli* standard collection of reference and express different amounts of α-haemolysin (Lai *et al.*, 1999). Vesicle preparations from the four strains were isolated and analysed (Fig. 8A). Immunoblot analysis using anti-α-haemolysin antisera confirmed the presence of α-haemolysin in the vesicles isolated from the four strains and haemolytic activity assays confirmed that the α-haemolysin in the OMVs was active (data not shown). Studies of the protein profile of the vesicles by detecting specific components of the outer and inner membranes indicated that the vesicles produced by these strains were in all cases OMVs (data not shown). Using the quantitative determination of OmpA by Western blot as an estimation of OMVs produced, the strains ER52, ER54 and ER60 produce apparently the same amount of OMVs. Interestingly the strain ER53 seems to produce a significant lower amount of OMVs (sixfold lower amount of OmpA was detected). The percentage of the soluble and OMVs-associated α-haemolysin was estimated and found to vary dependent on the strain. The average percentage of OMVs-associated α-haemolysin was 2.5%, 1.7%, 14.3% and 31.4% for the strains ER52, ER53, ER54 and ER60 respectively. The values were lower than in the case of strain MC1061 (66%) mentioned above but rather similar to estimates obtained with *E. coli* K-12 derivatives W3110 and MG1655 (17% and 11% respectively).

Outer membrane vesicles produced by the strain ER60 were visualized by atomic force microscopy (Fig. 8B). Similarly to what was described above for the α-haemolysin producing K-12 strains two types of vesicles were found: small vesicles with a diameter of approximately 50–70 nm and a minor subpopulation of larger vesicles with a diameter of 150–200 nm. We conclude that the features of OMVs from the laboratory strains are found also in the cases of natural and clinical *E. coli* isolates.

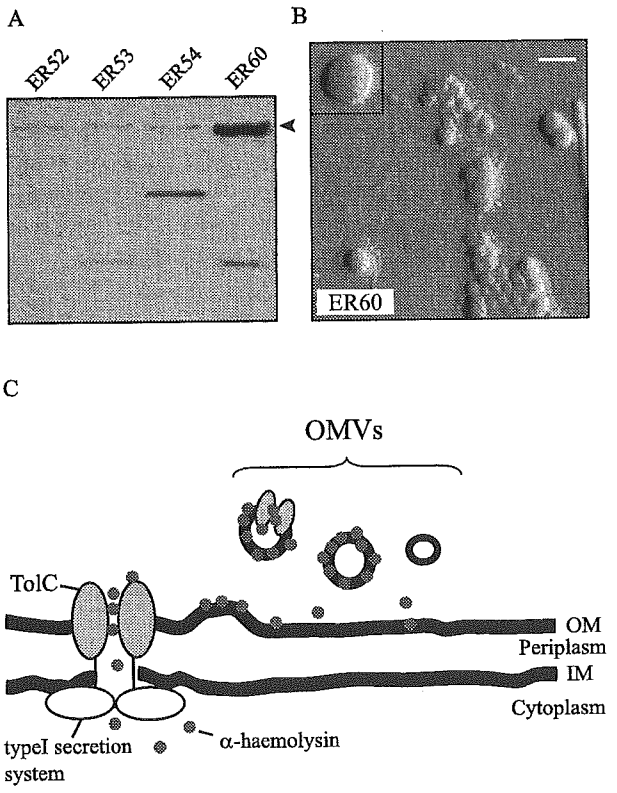

Fig. 8. The localization of α-haemolysin in OMVs is a common feature among haemolytic *E. coli* strains.
A. Immunoblot analysis of vesicles from the strains ER52, ER53, ER54 and ER60 using anti-α-haemolysin antisera. The band corresponding to the α-haemolysin is indicated with an arrowhead. In the gel the OMVs isolated from 10 ml supernatant of a culture with an OD_{600} of 0.8 were loaded.
B. Atomic force microscopy imaging of OMVs from strain ER60. The insert highlights an example of the larger vesicles in the preparation. Bar equals to 100 nm.
C. Model of secretion and OMVs localization of the α-haemolysin (see text).

Discussion

The secretion of the α-haemolysin is the prototype for the type I secretion system, a *sec*-independent system where the proteins are translocated in a one-step process to the extracellular media in a soluble form, without a periplasmic intermediate (see model in Fig. 8C). The present study establishes that a clearly recognizable fraction of the secreted α-haemolysin is, in fact, associated with OMVs. Analyses of the vesicle fraction by dissociation assays and density gradients showed that the α-haemolysin was tightly associated with the OMVs. Interestingly, OMVs fractionation and EM structural studies suggested that the OMVs containing α-haemolysin are characterized by their larger size, thinner margin and lower density when compared with the non-α-haemolysin containing OMVs. Moreover, our results showed that the protein composition was different between the two types of OMVs and we found that a type I machinery component, the TolC protein, was associated to the α-haemolysin containing OMVs. These results suggest that the α-haemolysin is preferentially localized in OMVs with a particular protein composition. Most of the experiments performed in this work were done in the *E. coli* strain MC1061, which was empirically chosen by being a high OMVs producer strain. The strain MC1061 is *galE*15 *galU galK*16 (Casadaban and Cohen, 1980), which might affect LPS composition. However, the localization of the α-haemolysin in OMVs was also observed in wild-type strains such as W3110 and MG1655 (Fig. 5 and C. Balsalobre, unpubl. data) and the ECOR strains (Fig. 8A), ruling out the possibility that the phenotype observed was unique for a particular strain. Tests with an *rfaG* mutant derivative of strain W3110 indi-

cated that a higher percentage of α-haemolysin was localized to the OMVs when compared with the wild-type isogenic strain (our unpublished data). Perhaps the LPS structure of the bacteria can influence the localization of the α-haemolysin. This could then be the reason for the observed differences with different natural isolates. Furthermore, that would also provide a possible explanation for the earlier reported phenotypes of rough LPS-producing strains that showed a decrease in the amount of active secreted α-haemolysin (Stanley *et al.*, 1993; Wandersman and Letoffe, 1993; Bauer and Welch, 1997).

The production of OMVs is a common phenomenon for most Gram-negative bacteria (Beveridge, 1999). The role of OMVs in export and targeting of bacterial toxins is an emerging new concept. It has been proposed that the heteromeric heat-labile enterotoxin (LT) produced by enterotoxigenic *E. coli* (ETEC), after it is secreted to the extracellular milieu by the general secretion pathway, is interacting with the LPS and released from the bacterial surface by OMVs (Horstman and Kuehn, 2002). Recently, it has been shown that an OMVs-mediated transport pathway is responsible for both (i) the export of the pore-forming cytolysin A (ClyA) from the bacteria and (ii) the activation of the ClyA cytotoxin by altering its redox status (Wai *et al.*, 2003). The mechanism of secretion of the α-haemolysin, by the periplasmic-independent type I pathway, differs completely from the toxins described above and there is no resemblance in protein sequence or structure. Our present results indicate that export of secreted proteins via OMVs not necessarily would require a periplasmic localization of the proteins during the secretion process. It seems likely that the protein transport to the extracellular milieu via OMVs may occur independently of the mechanism of protein secretion.

Our findings provide the first evidence that physiologically active α-haemolysin is associated with OMVs. However, the HlyC-mediated acylation, which is essential for the activity, was evidently not required for the localization of the α-haemolysin in the OMVs (Fig. 5). Previous studies have shown that the acylation of the α-haemolysin is not required for the stable association of the α-haemolysin with erythrocytes (Bauer and Welch, 1996; Moayeri and Welch, 1997). An intriguing question is whether the localization of the α-haemolysin in OMVs affects the activity of the toxin compared with the soluble form. At present, it is not possible for us to provide answer to this but we conclude that both forms were active. The well documented instability of the α-haemolysin (Welch, 1991) and the experimental design of the process of purification of OMVs did not allow us to quantitatively compare the activities of the two forms of the toxin.

A schematic model is summarized in Fig. 8C. An intriguing possibility is that formation of OMVs occasionally may occur where the type I secretion machinery is assembled. As a consequence, the α-haemolysin protein, perhaps together with some secretion system components (e.g. TolC), would be incorporated into the OMVs before leaving the bacterial cell. If so, the secretion system may affect the composition of the OMVs. At present we have no detailed information about the localization, topology and possible functional interactions of the proteins in the OMVs. Future studies will hopefully reveal if, e.g. TolC and/or other components are forming a type I secretion pore structure or if they may generate a special type of OMVs when localized with the Hly proteins. It will also be of interest to assess if accessory proteins like HlyB and/or HlyD are appearing in the OMVs.

All the results described here are compatible with the current model of how the α-haemolysin is translocated over the bacterial envelope when secreted by the type I secretion system from *E. coli*. Our findings are also consistent with the earlier reported observation that secreted α-haemolysin appeared to be localized on the surface of the bacteria (Oropeza-Wekerle *et al.*, 1989). After secretion to the extracellular space the α-haemolysin presumably binds to the bacterial surface and then it may be released in a relatively concentrated fashion by being associated with the OMVs. All our results obtained by different approaches (dissociation assays, proteinase susceptibility, immunogold labelling and the inability of externally added α-haemolysin to bind MC1061/pACYC184 OMVs) suggest that the α-haemolysin associated to the OMVs is not entirely exposed but somehow protected by the OMV structure (Fig. 2). No proteinase K digestion was detected when the vesicle structure was intact (no detergent added). Interestingly, an intense deposition of gold particles was only detected in areas where vesicles structures seemed disrupted. When intact vesicles were observed, little or no gold deposition was detected (Fig. 2E). These results are consistent with the suggestion that the α-haemolysin in the intact vesicles is not exposed and was only recognized by the monoclonal antibody when disruption of the vesicle structure had occurred.

Our results obtained by both biochemical and microscopy methods suggested a localization of the α-haemolysin not much exposed on the surface of the OMVs when we studied native samples of (i.e. non-fixed) OMVs. In the work by Oropeza-Wekerle *et al.* (1989), the α-haemolysin was detected in association with the cell-membranes by using immunogold labelling with polyclonal anti-α-haemolysin antisera on glutaraldehyde-fixed cells. Methodological differences between these studies may explain the apparent differential degree of exposure of the toxin when associated with membranes.

Another type I secreted protein has been described to be associated to membrane vesicles, the leukotoxin of *Actinobacillus actinomycetemcomitans*. Characterization

